Downloaded from https://www.lyellcollection.org by Guest on Jul 10, 2025

JGS
Journal of the Geological Society

Research article

https://doi.org/10.1144/jgs2024-239 | Vol. 182 | 2025 | jgs2024-239

Basaltic fissure eruptions of the Mull lava field, British Paleogene Igneous Province

Jessica H. Pugsley[1]*, Malcolm J. Hole[1], David W. Jolley[1], John M. Millett[1,2], John A. Howell[1], Adrian Hartley[1], Ailsa K. Quirie[1,3], James Westland[4] and Natália Famelli[5]

[1] School of Geosciences, University of Aberdeen, Aberdeen, UK
[2] Volcanic Basin Energy Research AS, Oslo, Norway
[3] Shell Research Ltd, Silver Fin Building, 455 Union Street, Aberdeen, UK
[4] Mull Geology, Isle of Mull, UK
[5] Instituto de Geociências, Universidade Federal do Rio Grande do Sul, Rio Grande do Sul, Brazil
JHP, 0000-0002-2148-0002
*Correspondence: jessica.pugsley@abdn.ac.uk

Abstract: Linear fissure zones commonly feed modern basaltic eruptions, yet direct evidence for such fissure eruption sites within ancient large igneous provinces remains scarce. We present a detailed examination of a well-preserved sequence of vent-proximal basaltic deposits from the Isle of Mull within the British Paleogene Igneous Province. We interpret these deposits as a segment of a dissected dyke-fed fissure zone. By combining photogrammetry and fieldwork, we identify a >5 km coastal zone near Calgary Bay, Isle of Mull hosting eruption vent-proximal basaltic deposits. In two main locations, the pyroclastic deposits exceed 5 m in thickness and contain basaltic airfall tephra, bombs and agglutinated spatter, in places forming spatter ramparts – features indicative of vent-proximal explosive basaltic activity. These deposits are intersected by numerous irregular intrusions with ragged edges, which terminate beneath the top surface of the pyroclastic layers, suggesting a complex network of partially drained feeder dykes. Vent-proximal effusive basaltic lava deposits in the area include agglutinated clastogenic lavas, spongy pahoehoe, inflated pahoehoe and, less commonly, ‘a‘ā lavas, along with multiple instances of lava tubes. This study provides novel insights into the eruptive architecture and processes within the North Atlantic Igneous Province, documenting a previously uncharacterized dissected large igneous province fissure system.

Received 4 November 2024; **revised** 31 March 2025; **accepted** 7 April 2025

Fissure-fed basaltic lava flows and pyroclastic eruptions are characteristic features of modern basaltic volcanic fields. However, outcrop exposures of fissure zones are comparatively rare in the geological record of large igneous provinces (LIPs), with a few notable exceptions (e.g. Mège and Korme 2004; Reidel 2015). Although fissure vent-proximal outcrops are seldom preserved within LIPs, dyke swarms are common and are often interpreted as the eroded remnants of fissure zone plumbing systems (e.g. Walker 1995). Examples include the Nandurbar–Dhule dyke swarm of the Deccan Traps, India, inferred to be the feeder system for the Jawhar–Igatpuri lava flows, and the Chief Joseph dyke swarm, which is thought to have fed the Grande Ronde basalt flows of the Columbia River Basalt Province in the USA (Reidel and Tolan 1992).

The scarcity of LIP fissure exposures may result from palaeoerosion, the emptying of feeder dykes, later overprinting by subsequent intrusions or a combination of these processes. In addition, fissures typically occupy a smaller area than the associated lava fields and therefore have a reduced likelihood of exposure and preservation. Nonetheless, the identification and systematic analysis of exposed fissure sites can yield valuable insights into eruption dynamics, distribution, longevity, magma–host rock interactions and the palaeoenvironmental impacts of LIP eruptions (Carey and Sparks 1986; Stothers *et al.* 1986; Wilson and Walker 1987; Pyle 1989; Parfitt and Wilson 1999; Houghton *et al.* 2006; Brown *et al.* 2015; Black *et al.* 2021).

Notable examples of vent-proximal deposits within LIPs include the well-documented Ice Harbor flow field in the Columbia River Basalt Group, where pyroclastic features (such as cones, scoria sheets, spatter-fed clastogenic lavas and bombs) have been identified (Swanson *et al.* 1975; Brown *et al.* 2015; Reidel 2015). Some Ice Harbor vent structures, however, are also interpreted as the result of rootless cone formation rather than as primary volcanic vent features (Brown *et al.* 2015; Reynolds *et al.* 2015). Columbia River Basalt Group exposures at Joseph Creek reveal deposits characteristic of Hawaiian-type eruptions, including tephra, localized lava flows, partially drained dykes and collapse breccias (Reidel and Tolan 1992). These Joseph Creek deposits represent a primary vent on a fissure system extending over 300 km (Reidel and Tolan 1992).

In subsurface records, 3D seismic imaging and well data show a 25 km long fissure zone with vents and vent-proximal lavas, as well as hyaloclastite deposits, in the Jurassic Rattray Volcanic Province, UK Central North Sea (Quirie *et al.* 2019, 2020). Similarly, in the Paleogene Faroe–Shetland Basin, linear palaeohighs surrounded by semi-radial lava flows indicate the presence of localized fissures (Schofield and Jolley 2013).

Modern basaltic fissure eruptions, by contrast, are often observed. Since 2021, multiple fissure eruptions on Iceland’s Reykjanes Peninsula have provided valuable insights into the development of fissure zones and their eruptive products (Büyükakpınar *et al.* 2025). Iceland also hosts numerous historical fissure systems, such as the 1783–84 Laki fissure eruption, where prolonged effusive activity produced >140 localized vents along a 27 km long fissure, with associated scoria, spatter, tephra and lava deposits (Thordarson and Self 1993). Similarly, fissure eruptions are common on Hawaii, including the longest recorded effusive event, the Pu‘u ‘Ō‘ō eruption of Kīlauea (1983–2018), which initially began as a discontinuous 7 km long fissure eruption before the activity localized to the Pu‘u ‘Ō‘ō vent (Garcia *et al.* 2021).

Within the British Paleogene Igneous Province (BPIP), most of the documented evidence for eruption sites originates from the

© 2025 The Author(s). This is an Open Access article distributed under the terms of the Creative Commons Attribution License (http://creativecommons.org/licenses/by/4.0/). Published by The Geological Society of London. Publishing disclaimer: https://www.lyellcollection.org/publishing-hub/publishing-ethics

Downloaded from https://www.lyellcollection.org by Guest on Jul 10, 2025

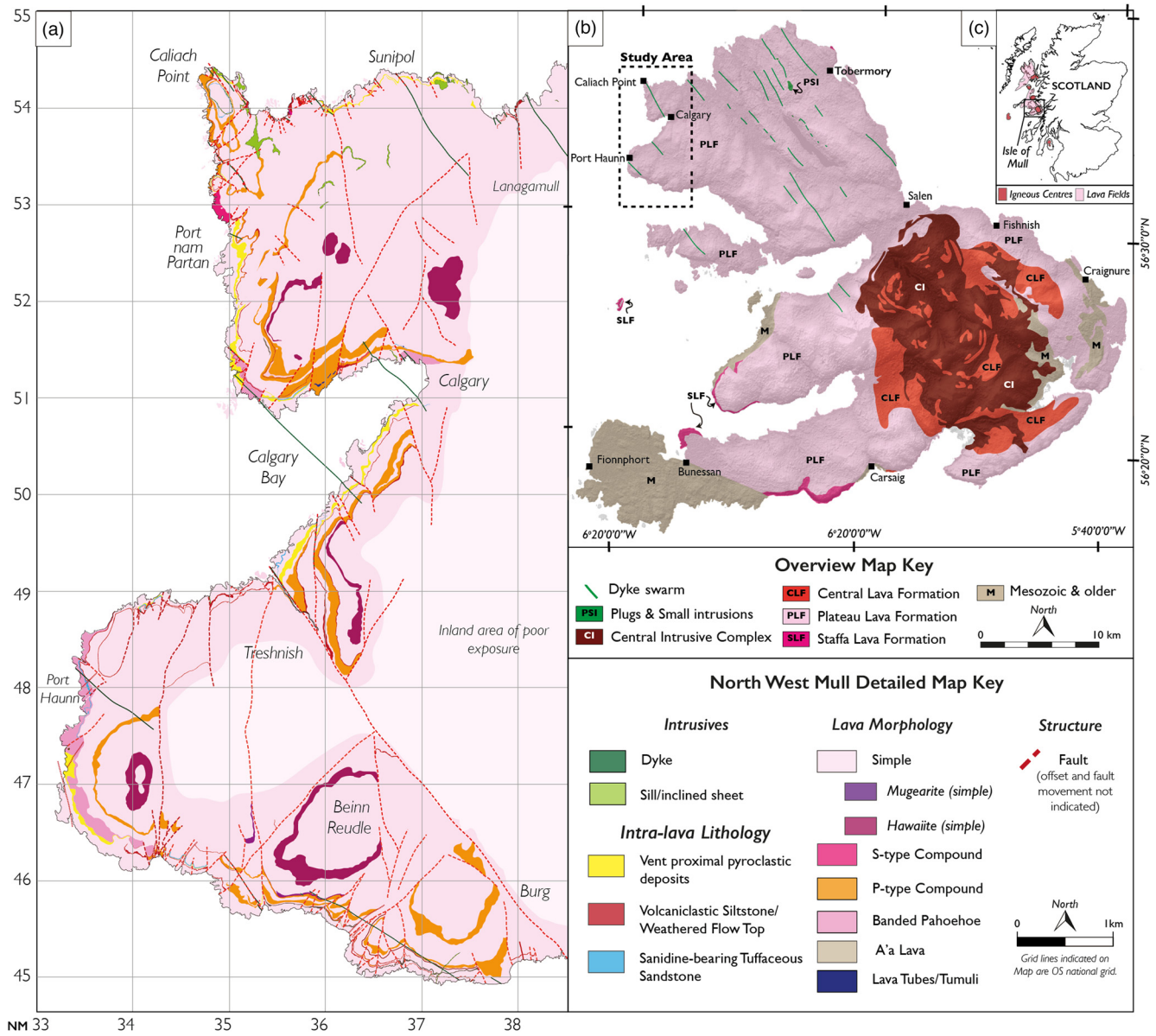

Fig. 1. (**a**) Geological map of study area (1:50 00 scale) and showing a simplified, not significant, level of structural complexity. (**b**) Map of the Isle of Mull showing the basic geology of the island and the location of the study area. (**c**) Location of the Isle of Mull in Scotland, UK, indicating the volcanic centres and lava fields.

plumbing systems associated with large central volcanoes (Bailey *et al.* 1924; Emeleus and Bell 2005) and extensive dyke swarms, which are hypothesized to have supplied now-eroded fissure zones (Macdonald *et al.* 2015). This led to considerable debate in the late nineteenth century regarding the origins of the lava sequences (Walker 1995): one model advocated a fissure-fed eruption style (Geike 1871, 1894) and the other a model in which the eruption was fed by a central complex (Judd 1886, 1889). Direct evidence for fissure eruptions within the BPIP, beyond systems inferred to be fed by dyke swarms, remains limited.

This study documents a previously unrecognized, exceptionally well-preserved and intricately dissected dyke-fed fissure zone within the Mull lava field of the BPIP, part of the North Atlantic Igneous Province (NAIP). This fissure zone reveals partially drained feeder intrusions, extensive vent-proximal pyroclastic deposits and a range of effusive lava facies. To our knowledge, this is the first detailed account of a potentially widespread basaltic fissure zone within the BPIP.

Previous studies on Mull have identified some evidence suggestive of local fissure eruption sources. Bell and Williamson (2017) documented a linear zone of foliated basalt in the Quinish lava flow, which they interpreted as possibly indicative of a feeder fissure structure. Williamson and Bell (2012) reported accumulations of spatter and pyroclasts in the Staffa Lava Formation, which may be evidence of vent-proximal deposits. Famelli *et al.* (2021) described local rootless cones and phreatic deposits at Carraig Mhor. Potential vent-proximal eruptive deposits have also been documented by Brown and Bell (2007) and Millett *et al.* (2024), providing further evidence for fissure-fed systems within the BPIP. Our study builds on previously published studies and presents new empirical support for the fissure-fed model commonly proposed for this region's lava sequences – a subject of debate for more than 150 years (e.g. Geike 1871, 1894; Judd 1886, 1889; Bailey *et al.* 1924; Kent *et al.* 1998; Emeleus and Bell 2005; Williamson and Bell 2012).

Geological setting

The BPIP presents some of the earliest igneous activity of the NAIP, which is commonly attributed to the presence of an active thermal anomaly during the early Paleogene (e.g. Skogseid *et al.* 1992;

Downloaded from https://www.lyellcollection.org by Guest on Jul 10, 2025

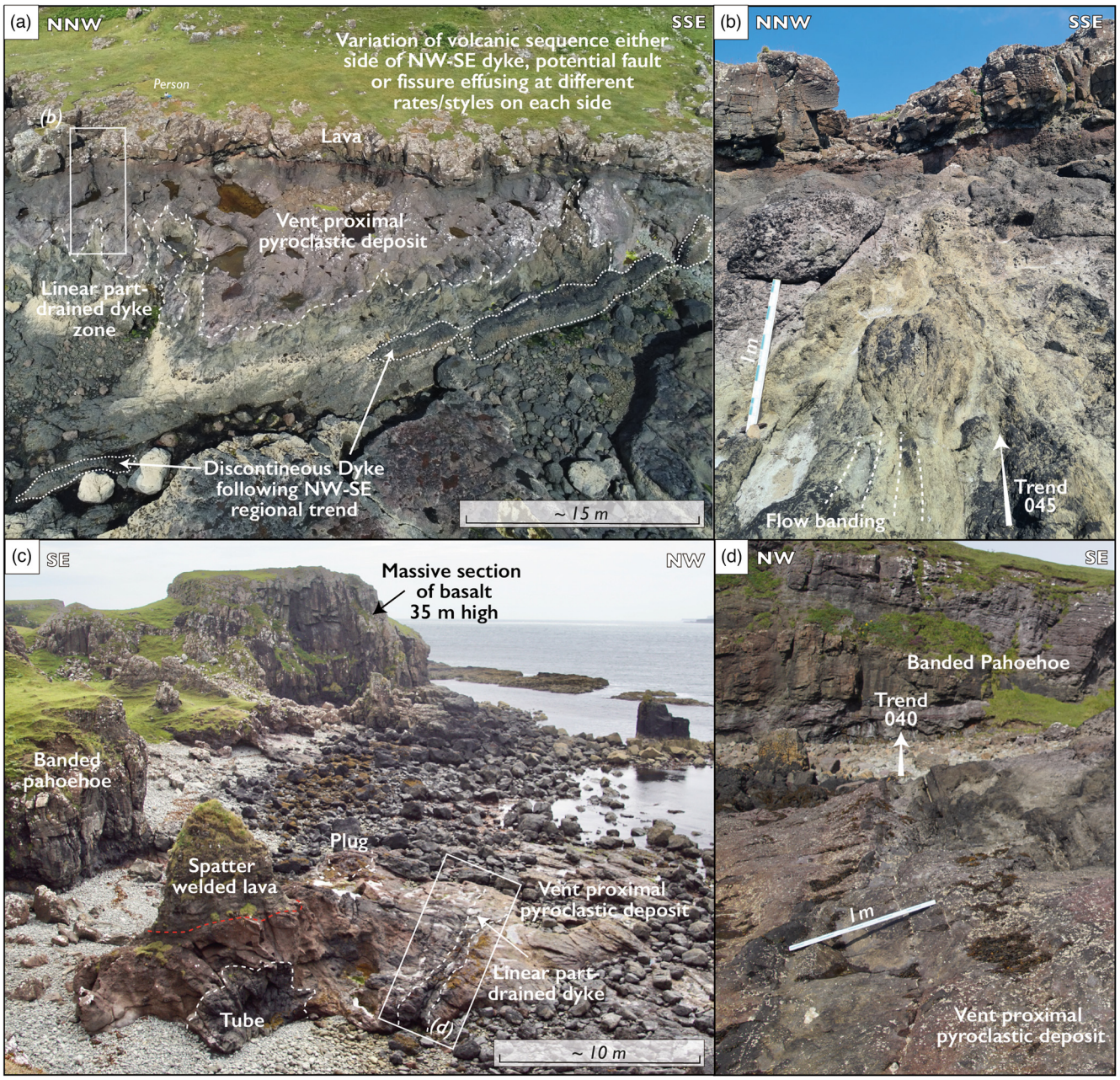

Fig. 2. Exposures of vent-proximal deposits. (**a**) NW Calgary Bay [NM 3506 5151], irregular ragged network of dykes terminating within a vent-proximal pyroclastic deposit consisting of basaltic tephra, including cow-dung bombs. (**b**) Termination of a ragged dyke illustrating its gradational transition into a pyroclastic deposit, likely a result of fluid movement and intrusion into an unconsolidated scoria, and near-vertical flow banding within dyke. (**c**) Network of irregular intrusions through pyroclastic deposits, including dykes, tubes and plugs at Port Haunn [NM 3336 4718]. The pyroclastic unit consists of basaltic tephra, vent-proximal spatter and overlying spatter-welded clastogenic lavas. (**d**) Irregular dyke with ragged margin intruding through a pyroclastic deposit; the irregular thickness may be a result of partial draining. The dyke is not seen to cross-cut any of the overlying lavas.

White 1993; Ritchie and Hitchin 1996; Kent and Fitton 2000; Emeleus and Bell 2005; Millett *et al.* 2016). The BPIP formed at the fringes of the NAIP, several hundred kilometres south of the eventual axis of continental break-up between Europe and East Greenland (Mihalffy *et al.* 2008; Shorttle *et al.* 2014; Hole *et al.* 2015). The Isle of Mull Paleogene volcanics, part of the BPIP, are mainly hosted within the Northern Highland Terrane (Bailey *et al.* 1924). The Mull volcanism was erupted onto the eroded Mesozoic stratigraphy and, in places, potentially over the Neoproterozoic metasedimentary basement (Bailey *et al.* 1924; Holdsworth *et al.* 1987; Emeleus and Bell 2005).

During the Caledonian Orogeny, a series of NE–SW-trending shear zones and faults formed, which established a long-lived structural grain within the Inner Hebridean region (Jacques and Reavy 1994). During the late Caledonian Orogeny, several granitic plutons were also emplaced within the Inner Hebrides; the Ross of Mull granite in SW Mull, for example, intruded the Moine metasedimentary strata (Haliday *et al.* 1979). The Inner Hebrides were later subjected to a period of continental rifting, likely initiated during the Triassic, which exploited the earlier Caledonian fabric and formed a series of NW–SE-trending half-graben and graben (Watson 1977; Hesselbo *et al.* 1998). The intrusive dykes that likely fed the extrusive volcanism harnessed pre-existing lineaments, which, in turn, exploited this inherited fabric (Watson 1977; Jacques and Reavy 1994; Hesselbo *et al.* 1998; Archer *et al.* 2005; Fyfe *et al.* 2021).

The Mull lava field forms the majority (*c.* 670 km^2) of the bedrock geology of the Isle of Mull (Fig. 1) and extends to several

Downloaded from https://www.lyellcollection.org by Guest on Jul 10, 2025

small islands to the west of Mull (e.g. Eorsa, Ulva, Gometra, the Treshnish Isles and Staffa), Morvern and eastern Ardnamurchan (*c.* 830 km^2 in total). The mountain of Ben More exhibits the thickest continuous sequence of lavas from sea-level to 966 m; this is a minimum value as neither an upper nor lower contact is exposed (Richey 1961). It is believed the total preserved thickness of lavas on Mull is *c.* 1800 m (Emeleus and Bell 2005) and it is estimated, based on zeolite assemblages, that the total thickness of the lava prior to erosion may have been 2200 m (Walker 1971). The base of the volcanic sequence is rarely exposed, with examples including at Gribun, Carsaig and Bloody Bay, where the lavas lie unconformably on Mesozoic strata (Emeleus and Bell 2005). The presence of psammite (Moine), chert (Turonian 'Flint') and arkosic sandstone (Torridonian) clasts within the Lagganulva conglomerate also suggests that they, or associated deposits, were exposed during its deposition (Pugsley 2021).

The Mull lava field has been separated into three main lava formations based on the geochemistry, petrography and physical field-based observations. In general, the Staffa Lava Formation forms the lowermost units, which are overlain by the Plateau Lava Formation, which, in turn, is overlain by the Central Lava Formation, although some intercalation does occur between the formations (Kerr *et al.* 1999; Emeleus and Bell 2005; Williamson and Bell 2012; Jolley *et al.* 2023). Recent work has found examples of the Plateau Lava Formation type chemistry below the Staffa Lava Formation at Malcolm's Point (Jolley *et al.* 2023), illustrating the structural and geochemical complexity of the stratigraphy.

The Plateau Lava Formation includes *c.* 620 km^2 of exposed bedrock of the Isle of Mull, including in the study area. Research by Kerr (1993, 1995, 1997), Hole *et al.* (2023) and Jolley *et al.* (2023) has provided insights into the complex geochemical evolution of Mull. Although dykes of Plateau Lava Formation composition have previously been identified in the Mull Central Complex (Macdonald *et al.* 2015), there is no documented evidence of feeder dykes reaching a palaeosurface – that is, no direct observation of fissure-fed volcanism. The study area of NW Mull is entirely formed of the Plateau Lava Formation (Pugsley 2021; Hole *et al.* 2023), which presents a large range in lava morphologies and geochemical variation, along with significant structural complexity (Fig. 1a).

Methods

The geological exposures in NW Mull are primarily composed of continuous coastal cliffs, ranging from 20 to 35 m in height, with generally good accessibility. The inland exposures are largely limited to the erosion-resistant cores of larger simple lava flows. This study involved extensive field mapping, stratigraphic logging and systematic sampling. Photogrammetry was used to generate virtual outcrops, supplementing the fieldwork and enabling analysis of otherwise inaccessible cliff sections through the following workflow.

- *Model collection*. Imagery was captured using DJI Phantom 3 Pro, DJI Phantom 4 and DJI Phantom 4 Pro drones, flown *c.* 15–30 m from cliff sections for the detailed models and 30–80 m for broader overviews (following Howell *et al.* 2021). Several thousand images, covering *c.*18 km of coastline from Sunipol to SE Beinn Reudel, were collected for virtual outcrop construction.
- *Model processing and virtual outcrop construction*. Agisoft PhotoScan software was used to process the images and construct virtual outcrops as .obj files (see Buckley *et al.* 2008; Kehl *et al.* 2016).
- *Virtual outcrop interpretation*. The .obj files were imported into LIME software, where tools such as lines, panels and planes facilitated the interpretation of the virtual models, which were then calibrated against the field data and samples (following Buckley *et al.* 2019).
- *Virtual outcrop distribution.* The virtual outcrop models referenced in this study are accessible via the v3Geo viewer (https://www.v3Geo.com) (see Buckley *et al.* 2021).

Virtual outcrops were essential to this study, providing high-resolution spatial data and supplementing the field-based interpretations.

Results

We document a Paleogene fissure-fed lava field from NW Mull. The fissure system includes: (1) vent-proximal pyroclastic deposits; (2) dykes and other minor intrusions; and (3) diverse fissure-fed lava flow facies. The primary volcaniclastic and epiclastic deposits were described with reference to published classification schemes (Wentworth 1922; Fisher 1961; Cas and Wright 1991; Gillespie and Styles 1999). We applied the Gillespie and Styles (1999) classification for lava crystallinity.

Vent-proximal deposits of NW Mull

Pyroclastic deposits

Extensive outcrops of basaltic pyroclastic tephra and spatter deposits are exposed in several locations across the study area. Two main localities, Port Haunn [NM 3336 4718] (Fig. 2a, b) and NW Calgary Bay [NM 3506 5151] (Fig. 2b, c), exhibit type examples of these pyroclastic and intrusive interactions.

Both localities are exposed in the intertidal zone, on sea stacks and in sea cliffs, where they have comparable characteristics to those captured in the idealized log of Figure 3a. At Port Haunn, the deposit has a highly irregular top surface that undulates for more than its exposed thickness, which is >6 m because the base is not exposed. At NW Calgary Bay, a similar deposit has a relatively consistent top surface height with more gradual variations of 2–4 m in thickness. Across both localities, the pyroclastic units are dominantly composed of basaltic fragments with irregular lobate margins, which range in size from coarse grains (<1 cm diameter) to blocks and bombs (maximum *c.* 1 m diameter) (Fig. 3e).

At Calgary, the upper sections of the deposits are close-packed and clast-supported, forming non-welded scoria lapilli (Fig. 3c). The middle to lower section is a more matrix-supported pyroclastic deposit with evidence of crude bedding (Fig. 3g, i). The clasts are entirely volcanic, with varying crystallinity, colour and vesicularity, and the deposit varies from well to poorly sorted and includes cow-dung and fusiform bombs. The lobate margins, sinuous to fluidal shapes and often interlocking nature of the bombs, blocks and lapilli fragments indicate that they behaved plastically at the time of their initial deposition (MacDonald 1972; Fisher and Schmincke 1984; Holm 1987; Sánchez *et al.* 2012). Irregularly overlying these pyroclastic deposits are fine-grained tephra deposits up to 40 cm thick – for example, at [NM 3507 5149], which are red–orange in colour, fine to coarse grained (<0.5–1 cm) and highly weathered (Fig. 3b). The tephra is cemented by zeolites and predominantly composed of altered volcanic glass, with clear cuspate margins and vesicular structures when viewed in thin section.

At Port Haunn, similar tephra deposits are often passively invaded, or intercalated, by overlying spatter to welded spatter lavas, resulting in complex lava–tephra contacts. Here, the spatter to welded spatter lavas (Fig. 3f) typically overlie the tephra, followed by pahoehoe lavas with significant inflation-related banding described by Kent *et al.* (1998), termed banded pahoehoe within this study. By contrast, the overlying lavas at Calgary are typically compound to simple in nature with abundant horizontal tree fossils (moulds, casts and mineralogically replaced remnants) within their base. An exception occurs around the sea stacks at Rubha nan

Downloaded from https://www.lyellcollection.org by Guest on Jul 10, 2025

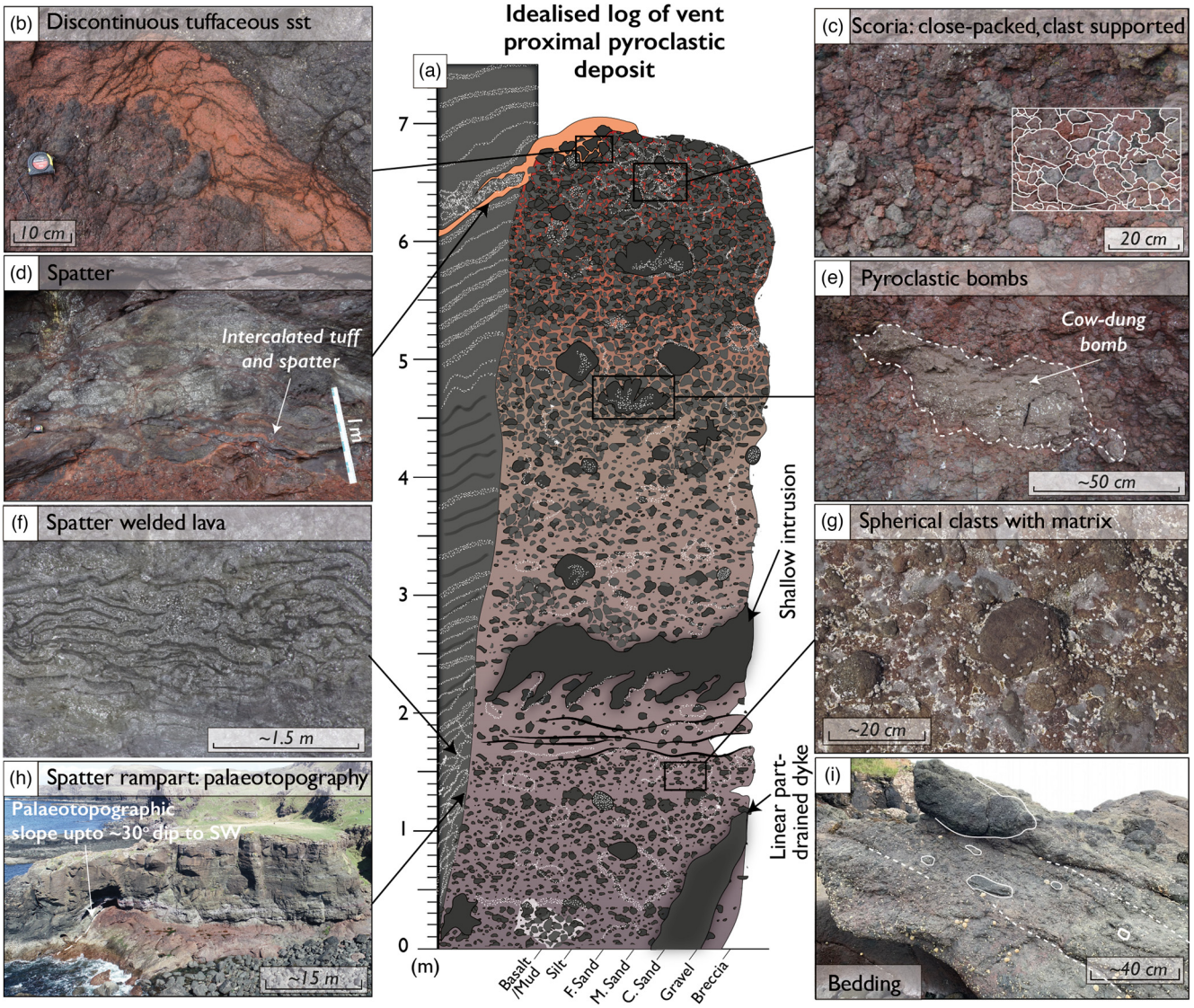

Fig. 3. Vent-proximal pyroclastic deposit exposed at Port Haunn and NW Calgary Bay. (**a**) Idealized log of the deposit at Port Haunn; most of the characteristics are found at both localities. (**b**) The discontinuous tuffaceous sandstone can present minor to no reworking. (**c**) Scoria, close-packed with little interstitial space between clasts. (**d**) Spatter stacked to form 1–2 m of chaotic vesicular blebs. (**e**) Pyroclastic deposit composed of airfall material, such as cow-dung (pie), breadcrust and fusiform bombs. (**f**) Spatter-welded lava forming more coherent, thin, lobe-like geometries (*c.* 20–30 cm thick). (**g**) Matrix (tuffaceous) supported section with spherical clasts with chilled margins. (**h**) Irregular palaeotopography forming a linear ridge through Port Haunn in a north–south orientation as a result of the development of a spatter rampart surrounding a fissure. (**i**) Scoria exhibiting bedding. sst, sandstone.

Oirean [NM 3515 5130], where a sequence strikingly similar to Port Haunn is exposed, including pyroclastic deposits overlain by spatter-welded lavas and banded pahoehoe lava.

Dykes and other shallow intrusions

Irregular shallow intrusions, with auto-brecciated, ragged margins, invade the pyroclastic deposits in the described localities (Fig. 2). At Calgary, the intrusions form a series of near-parallel ragged dykes with a general trend of 045° (NE) and they appear to amalgamate with depth. In most cases, the dykes terminate <1–3 m below the top of the vent-proximal tephra (e.g. Fig. 2a, b). The dykes exhibit near-vertical flow banding, including amygdaloidal bands. A columnar dyke following the regional NW–SE trend, discontinuous in exposure and intrusive in nature, irregularly intrudes through the pyroclastic rocks, but its relationship with the overlying lava is not clear (Fig. 2a).

At Port Haunn, the intrusions are more variable, forming dykes, sills, cylindrical sub-horizontal tubes and subvertical plugs. A dyke found within the wave-cut platform of a sea stack intrudes at a similar trend to the Calgary dykes at 040° (NE). The dyke is *c.* 1–2 m wide, non-vesicular and exhibits near-vertical fractures, flow banding and irregular fragmented margins, which appear to grade into the pyroclastic deposit. Within the base of the sea stack a distinct coherent 60 cm thick basaltic lens is exposed, laterally extending for >10 m. The lobe has small (*c.* 20 cm long) finger-like projections propagating from its base, which transition into juvenile clasts within the pyroclastic matrix in a northeasterly direction. The top of the lobe has an undulating smooth contact with the pyroclasts; however, within the limited exposure, the lobe is not seen to stem from the palaeosurface of the pyroclastic unit and therefore most likely formed as a shallow intrusion. To the SW of Port Haunn, a 35 m thick section of massive, generally non-vesicular, basalt (Fig. 2c) with prismatic jointing is juxtaposed against the surrounding banded pahoehoe lava.

Lava flow facies

Compound pahoehoe

Compound pahoehoe flows are lava formations that can be subdivided into multiple flow units (Walker 1971). In NW Mull,

Downloaded from https://www.lyellcollection.org by Guest on Jul 10, 2025

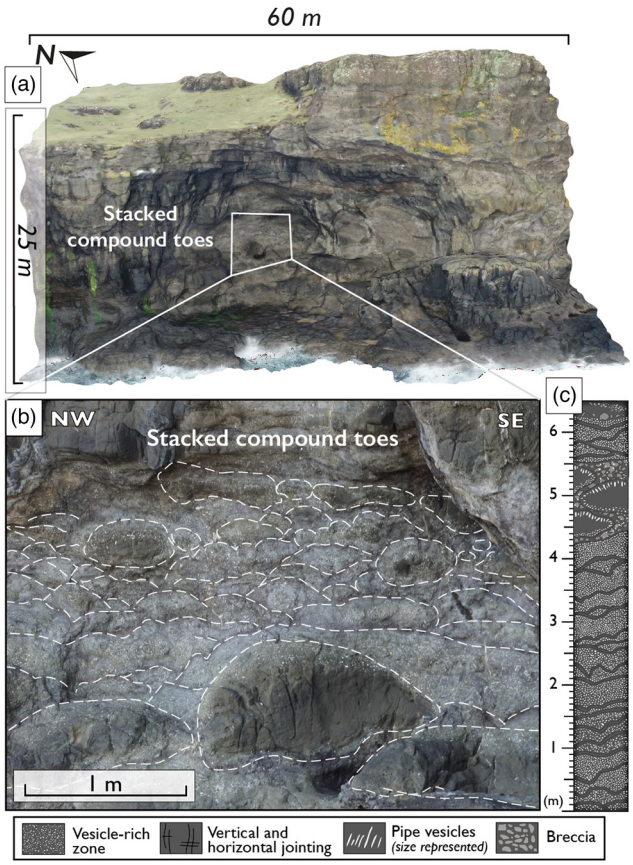

Fig. 4. Stacked sequence of small compound toes and lobes at [NM 3496 5203]. (**a**) Virtual outcrop displaying the >25 m sequence of stacked compound toes and lobes ranging from <1 m to >3 m thick and up to 3 m wide. (**b**) Field photograph from the same area with the lobe boundaries highlighted. (**c**) Idealized log of small compound toes and lobes.

stacked sequences of small compound lava lobes and toes are often poorly exposed due to their vesicular and amygdaloidal characteristics, leading to preferential erosion and vegetation cover. Where exposed, these sequences can reach thicknesses of 10–100 m.

Two primary forms of compound lava are identified: P-type (pipe-vesicle bearing; Fig. 4) and S-type (spongy; Fig. 5) pahoehoe, following the classification of Wilmoth (1993). Larger lobes typically exhibit P-type characteristics, featuring an amygdaloidal lower crust with occasional pipe vesicles measuring 2–10 cm, occasionally oriented in the flow direction. The lobe thickness varies from 0.5 to 10 m; some flows terminate after 10 m, whereas others exceed 100 m (Fig. 5).

The P-type lobes can be divided into three components: lower crust, core and upper crust. When the underlying substrate is irregular, the flows tend to infill gaps, resulting in a more irregular lower crust. The basal lobes may show poorly formed upper crusts associated with pahoehoe toe breakouts (Fig. 5b). The core is generally non-vesicular, with sporadic vesicle cylinders, vertical fractures and increasing crystal sizes toward the core. The upper crust has >40% amygdaloidal content, with amygdales that may exhibit grading or reverse grading; half-moon vesicles are commonly observed in the lower portions. Rare ropy structures can be noted at exposed flow tops, such as in the intertidal zone platforms (Fig. 5c).

Less commonly, extensive sequences of small compound lobes are observed, particularly along the cliffs north of Port nam Partan [NM 3496 5203] (Fig. 4). These lobes and toes, ranging from 0.5 to 1.5 m in thickness, are composed of S-type pahoehoe, characterized by a highly vesicular, spongy interior. The amygdales within S-type lobes range from 0.5 to 15 cm and can form up to 70% of the lobe volume, typically increasing in size towards the centre. The crusts are thin (0.5–5 cm), aphyric, dark grey and may show red or purple hues as a result of oxidation. Notably, P- and S-type compound lobes often coexist within the same stacked sequences.

Banded pahoehoe

Lava flows exhibiting extensive horizontal vesicle/amygdale zones (HVZs) in the upper crust and mineral flow banding in the core are classified as banded pahoehoe (Fig. 6). These lavas are primarily exposed in two locations: NW Calgary Bay [NM 3521 5112] and Treshnish, near Port Haunn [NM 3344 4753]. Banded pahoehoe is found overlying or closely associated with the previously described pyroclastic deposits (Fig. 3). A near-complete series of stacked banded pahoehoe lavas exists between Treshnish Point and the southern coast of Beinn Duill. However, due to discontinuous exposure, the regional stratigraphic tilt (2° NNE) and faulting, the exact number of individual lobes is uncertain, although a minimum of five flows can be distinguished.

The thickness of banded pahoehoe lobes ranges from <5 to *c.* 30 m, containing numerous small S-type and P-type lobes at [NM 33359 47295]. These flows display extensive HVZs in their upper crusts and mineral flow banding within the core, alternating between olivine-rich and olivine-poor bands at 30–150 mm intervals (Kent *et al.* 1998). The crystal sizes vary from aphanitic to coarse grained (up to *c.* 1 cm). Olivine-poor bands often show prominent pustular pyroxene weathering in outcrops away from wave erosion. Both brittle and plastic deformation are observed in the non-vesicular and HVZ layers (e.g. Figs 3f, 6d), likely relating to the temperature and cooling rates during lava movement. This deformation provides insights into the palaeoflow direction, which at [NM 33365 47300] is towards the NW (314°). The lowermost banded pahoehoe lobes exhibit the greatest variability in mineral flow banding and HVZ extent, intercalated with agglutinated lavas and compound lobes.

Simple lavas (sheet flows)

Simple lava is defined as lava that is not divisible into flow units (Walker 1971). These pahoehoe lavas exhibit a tabular, sheet-like geometry, characterized as flows with tabular-classic facies architecture (Jerram *et al.* 2002; Passey and Bell 2007). On Mull, the basal crust displays disordered fracture and vesicle patterns, with rare pipe vesicles, pockets of peperite and horizontal tree moulds. By contrast, the flow cores are dense and non-vesicular, predominantly featuring crude prismatic jointing, with only one example of columnar jointing, akin to those found in the older Staffa Lava Formation (Williamson and Bell 2012; Jolley *et al.* 2023) exposed south of Beinn Reudle (Fig. 7a). The upper crust contains the highest concentration of amygdales, which exhibit gradation and reverse gradation in weakly developed, laterally continuous vesicular zones. Some flow tops transition into rubbly flow tops, ranging from 0.5 to 4 m thick, indicative of transitional lava flow development. Occasionally, mineral flow banding is observed within the cores, primarily in hawaiite or mugearite compositions, although this banding is less developed than in the inflated banded pahoehoe cores described previously.

ʻAʻā lavas

In the cliffs south of Àrd Dubh Bhurg [NM 3689 4516], a 3–6 m thick sheet of aphyric basalt is encased within breccia 1–4 m thick, showing a lateral extent of *c.* 2 km. The aphyric basalt represents the core of an ʻaʻā lava, with the adjacent breccia corresponding to the rubbly clinker forming both the flow top and base (Fig. 8). This section traverses several minor faults. The transition from the

Downloaded from https://www.lyellcollection.org by Guest on Jul 10, 2025

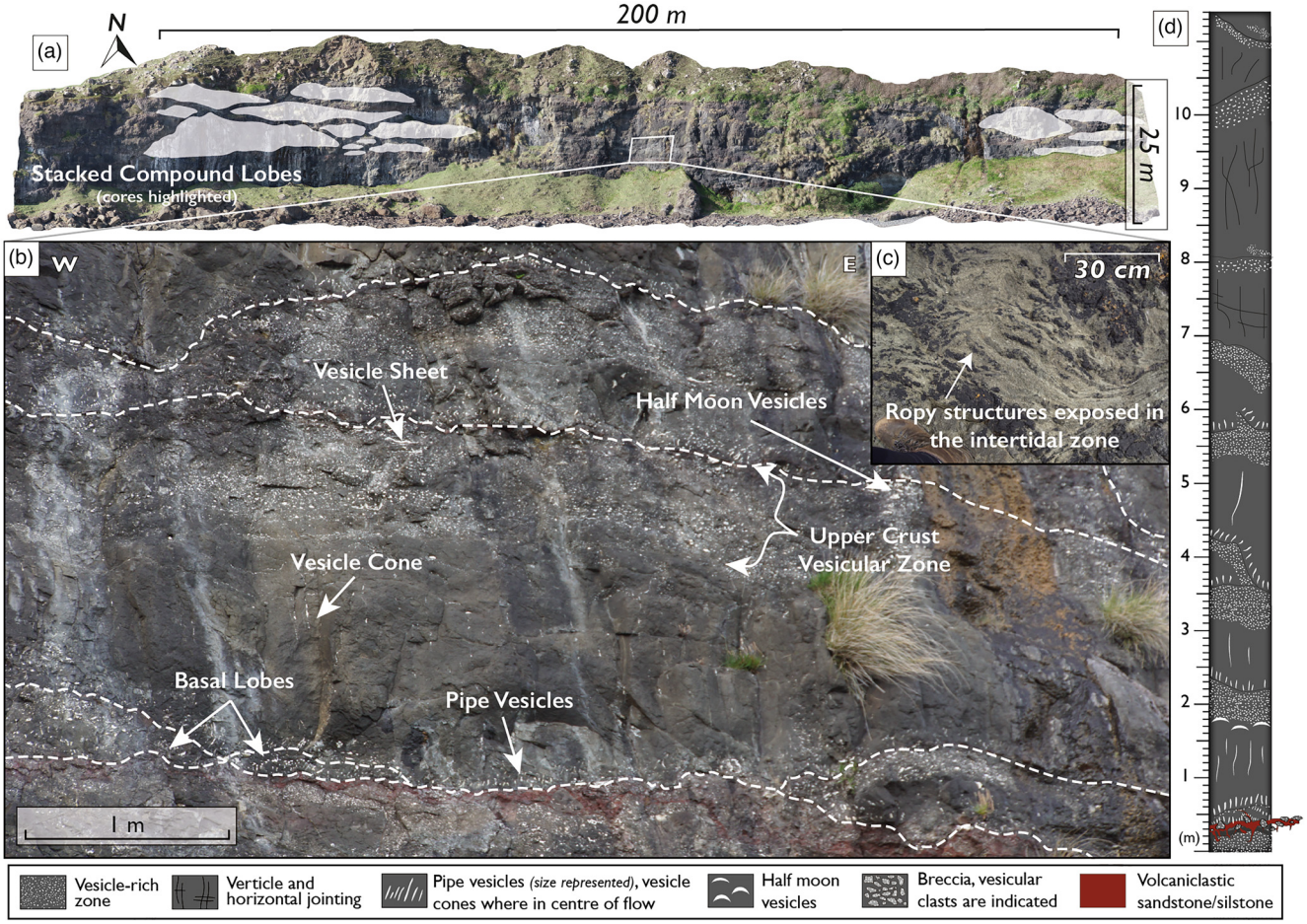

Fig. 5. Examples of stacked compound lobes with clear pahoehoe structures from the base of Beinn Reudel [NM 3556 4573]. (**a**) Virtual outcrop with some lobes highlighted; note that the stacked lobes form the entire cliff. (**b**) Field photograph of cliff highlighting the internal pahoehoe flow features. (**c**) Field photograph of ropy pahoehoe flow surface feature [NM 3540 4575]. (**d**) Idealized log of P-type compound lobes.

aphyric basalt flow core to the brecciated flow margin displays significant irregularities, characterized by lobate features. The breccia is poorly sorted and variable, ranging from clast-supported to matrix-supported textures; however, the exposure quality is limited, indicating possible alteration of the deposits. Clast sizes range from *c.* 1 to 40 cm, predominantly consisting of angular fragments with irregular margins, many of which are amygdaloidal in nature. Distinction between the clasts and the surrounding matrix is often challenging, particularly in regions exhibiting honeycomb and pock-marked weathering textures.

In the lower breccia, notable lenses of aphyric basalt with irregular margins are exposed, varying in thickness from <1 to 7 m. In rarer instances within the upper breccia, vertical, rounded protrusions or 'fingers' of basalt penetrate the breccia. The lower basalt lenses likely formed as invasive lava lobes during the same eruptive event. In addition, smaller 'a'ā flows, measuring <3 m in thickness and exhibiting laterally restricted distributions, are present in various locations associated with steep, lava-derived topography.

Invasive lava/shallow intrusions

Invasive lava refers to surface lava flows that laterally migrate into the subsurface, resembling shallow sills, while shallow intrusions remain entirely subsurface (Byerly and Swanson 1978; Hooper 1997; Rawlings *et al.* 1999; Famelli *et al.* 2021). On Mull and elsewhere, distinguishing between invasive flows and shallow intrusions can be challenging in areas of partial exposure. Invasive lavas and shallow intrusions are commonly found within the volcaniclastic and pyroclastic deposits of NW Mull (Fig. 9).

At Port Haunn, a shallow intrusion (Fig. 9a) within the vent-proximal pyroclastic unit described earlier shows no evidence of being fed by an overlying lava. Conversely, along a 1 km stretch of coastal cliffs at the southern base of Beinn Reudle, several invasive lava lobes intrude into a pyroclastic unit, connecting to a parent lava flow. For instance, at [NM 35882 45741], two stacked apophyses invade a rubbly unit, composed of broken pahoehoe lobes and vesicular cuspate clasts, which forms a palaeotopographic high that increases in elevation by 3–4 m (Fig. 9b, c). The upper invasive lobe extends 3.5 m into the volcaniclastic unit. The lobe is 1 m thick and features a chilled contact and three to five concentric amygdaloidal vesicle bands parallel to the lobe's edge. Individual amygdales typically measure <1 cm, coalescing in the core, which contains small vesicles (<0.5 cm). A rounded tip 15 cm from the lobe's tip features a circular lens of lava with a similar chilled contact and vesicular core, likely part of the same lobe (Fig. 9c). The lower invasive lobe is a non-vesicular, irregular lens of aphyric basalt that does not connect to the parent flow at the exposure, but was likely connected in 3D space. Bailey *et al.* (1924) described features termed 'auto-intrusions' along the southern shores of Beinn Reudle, which closely resemble the upper invasive lobe. Kent *et al.* (1998) suggested that these 'auto-intrusions' might refer to potential lava tubes at the base of Beinn Reudle, which were not observed in this study. Instead, we interpret the term 'auto-intrusion' used by Bailey *et al.* (1924) to mean invasive lava in this instance.

At the base of Beinn Reudle, another example of invasive lava connecting to a parent flow is exposed at [NM 36120 45600], where an invasive lava lobe bifurcates the brecciated unit (Fig. 10a). This outcrop appears to contain two rubbly horizons, likely pyroclastic;

Downloaded from https://www.lyellcollection.org by Guest on Jul 10, 2025

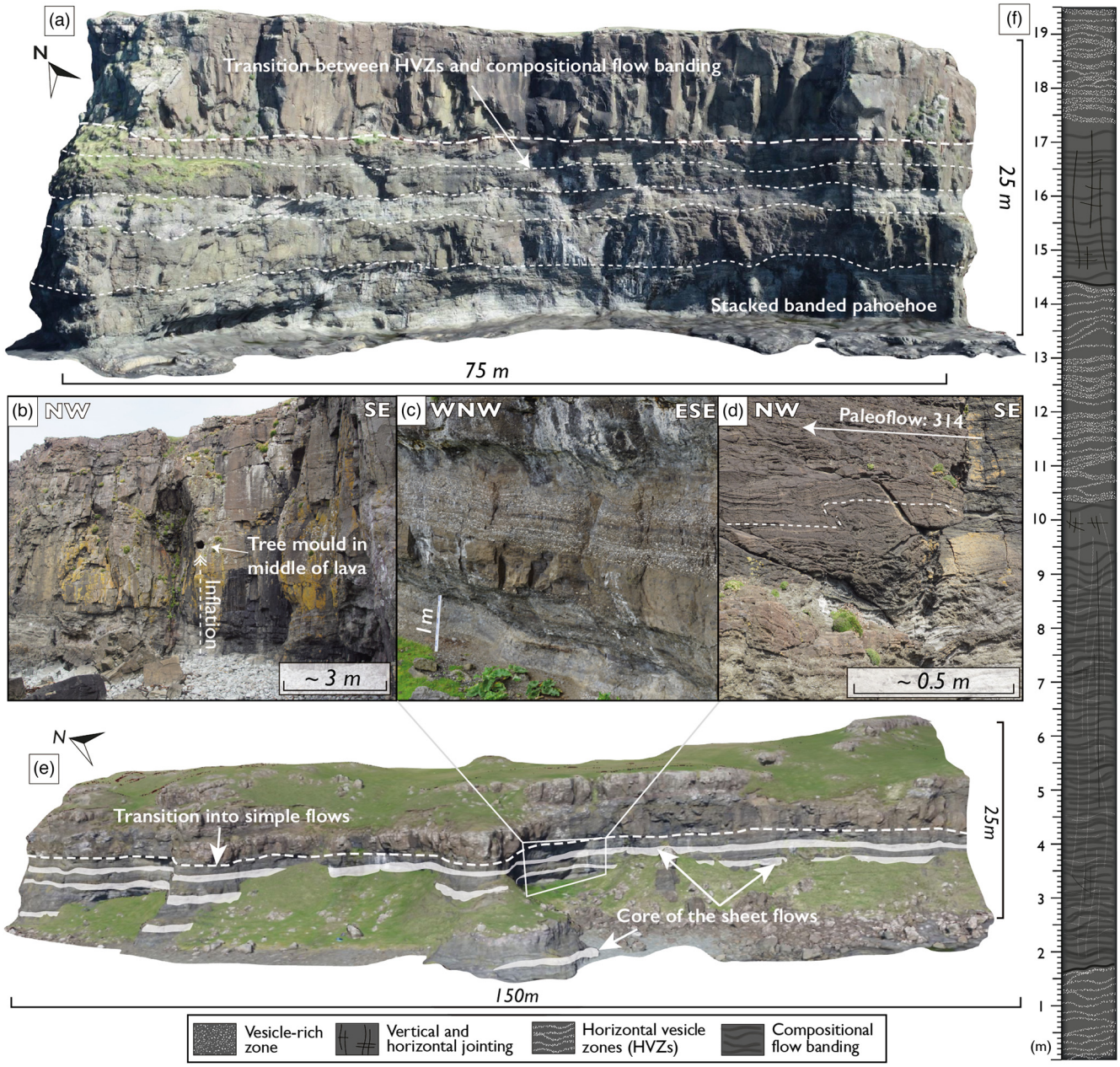

Fig. 6. Sheet flows illustrating extensive horizontal vesicle zones and flow banding within the core. (**a**) Virtual outcrop illustrating alternation between non-vesicular flow banding and horizontal vesicle/amygdale zones near Treshnish Point [NM 3355 4839]. (**b**) Tree fossil (mould) within core of flow *c.* 5 m above the base. This is a potential indicator of inflation. (**c**) Smaller example of a flow with laterally continuous and well-developed horizontal vesicle/amygdale zones. (**d**) Shear deformation forming a fault-propagated fold within the olivine-poor/olivine-rich banding. (**e**) Virtual outcrop illustrating thinner, although still laterally continuous, sheet flows with horizontal vesicle/amygdale zones at Rubha nan Oriean [N529 5119]. (**f**) Idealized log of lavas with extensive horizontal vesicle/amygdale zones and flow banding.

however, tracing laterally reveals a single vertical column between the two. Again, Bailey *et al.* (1924) described this as an 'auto-intrusion'. Walker and Cortés (2024) documented this exposure, describing it as a pahoehoe lava with multiple vesicular zones with 'mega vesicles', which we interpret as irregular surface weathering of the amygdaloidal clasts within the pyroclastic unit. Clasts within the vertical column and upper pyroclastic unit show signs of baking due to the effects of the invasive lobe. A cross-section of a second invasive lobe, suspended within a rubbly unit, forms a laterally confined sheet-like structure, 4.5 m thick and 25 m long, which has crude prismatic jointing, minimal vesicles and poorly developed chilled margins. To the west, the upper section of volcaniclastic material tapers and terminates within the parent lava flow. On the opposite side of the gully, additional invasive lobes are present within the same pyroclastic unit (Fig. 10b). To the east, distinguishing subaerial lava from invasive lava becomes increasingly difficult due to limited exposure. Across the study area, several more examples of potentially invasive lavas are observed, but their differentiation from shallow intrusions and potential 'a'ā lavas is complicated by poor exposure.

Lava tubes

Across the NW of the Mull lava field, lava tubes are present within sequences of compound lobes (Fig. 11). Where observed, the tubes are filled with lava and identified from their joint and amygdale patterns and relationship with the surrounding lobes. The larger of the two tubes exposed in the sea cliff south of Caliach Point [NM 3480 5395] (Fig. 11a) has a diameter of 11.9 m, an area of *c.* 116 m^2 and a trend of 075°. This tube has resisted weathering compared

Downloaded from https://www.lyellcollection.org by Guest on Jul 10, 2025

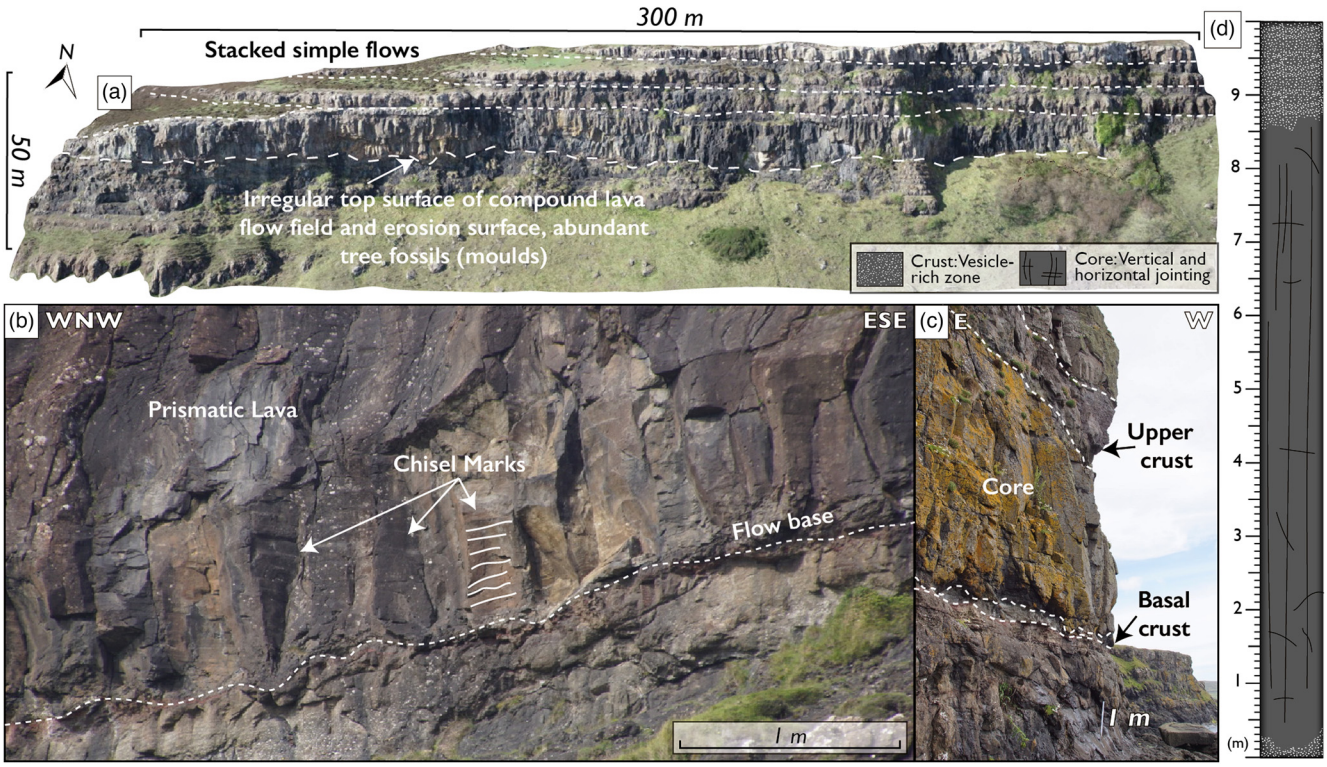

Fig. 7. Range of jointing within simple lava flows across the Mull lava field. (**a**) Sequence of stacked simple lava flows with the lowermost presenting well-developed vertical columnar joining [NM 3565 4586]. (**b**) Base of another simple lava flow with well-developed vertical fractures and horizonal chisel marks; the vertical fractures dissipate within the core and upper crust of the lava flow [NM 3366 4680]. (**c**) Simple lava flow presenting the typical expression of simple lava flows across NW Mull with a basal crust, core (with some vertical fractures) and upper crust (typically vesicular) [NM 3409 5205]. (**d**) Idealized log of a simple lava flow.

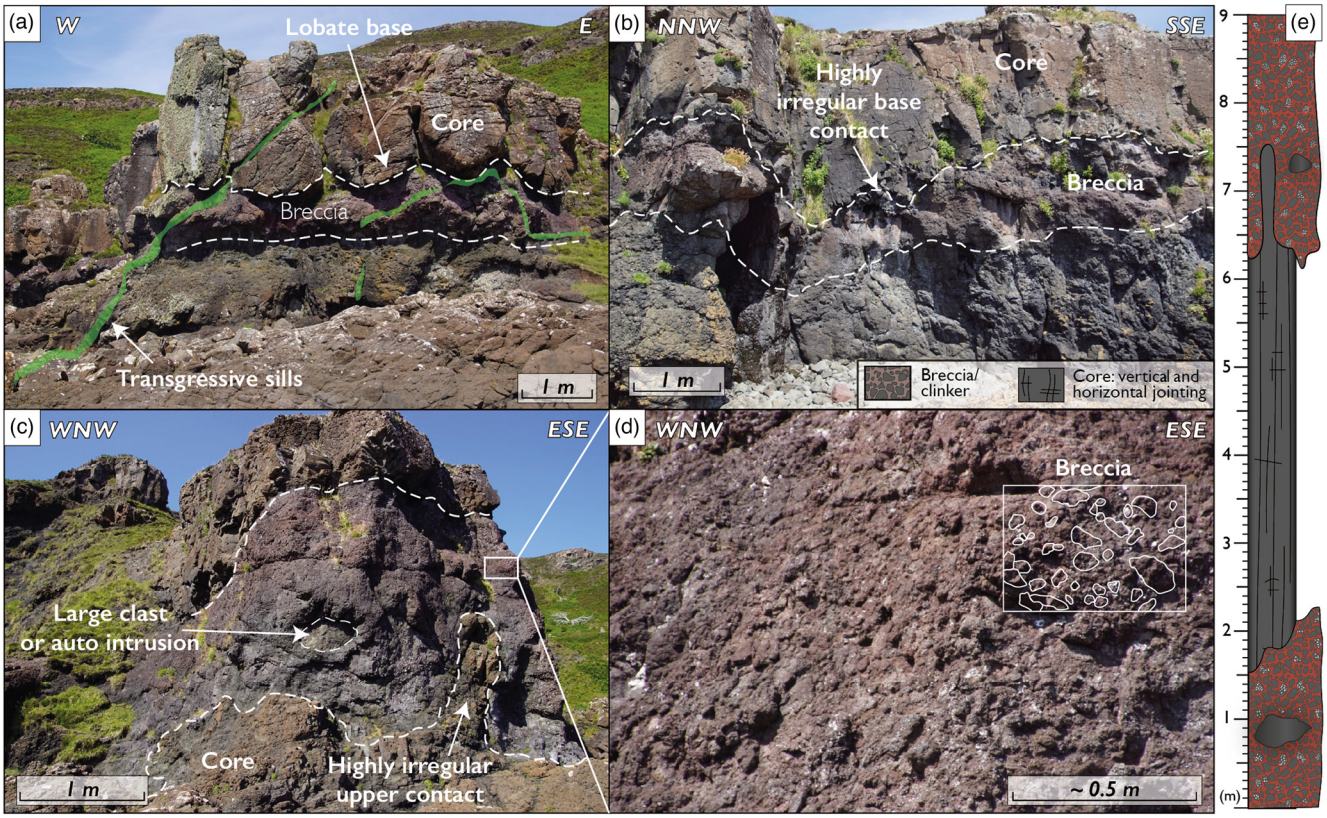

Fig. 8. Example of an ‘a‘ā lava flow exposed along the southern shore of Àrd Dubh Bhurg [NM 3689 4516]. (**a**, **b**) Lobate and irregular basal contact between the flow core and the lower breccia/clinker. (**c**) Highly irregular upper contact between the lava core and breccia/clinker top. (**d**) Brecciated texture of clinker, illustrating the range of clast size and vesicularity. (**e**) Idealized log of an ‘a‘ā lava flow.

Downloaded from https://www.lyellcollection.org by Guest on Jul 10, 2025

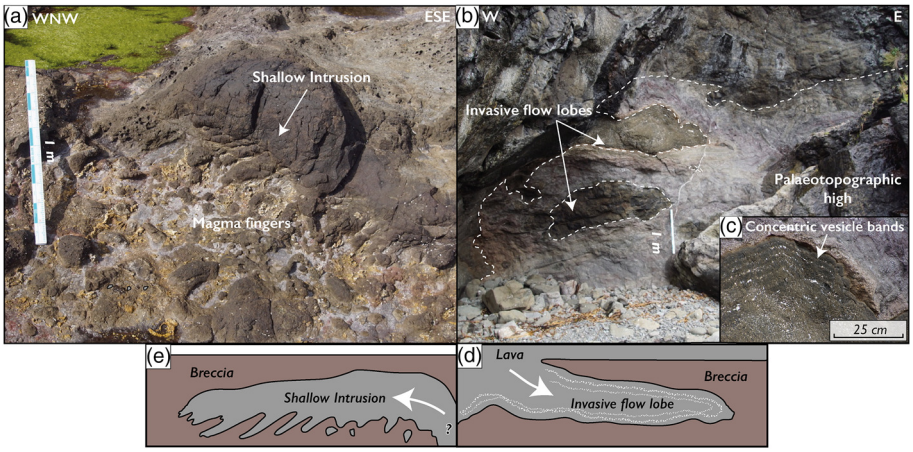

Fig. 9. Invasive lava/shallow intrusion within the volcaniclastic and pyroclastic units. (**a**) Flow toe with finger-like invasive branches leading into the tephra below. (**b**, **c**) Invasive lava lobes within a volcaniclastic palaeohorizon. The volcaniclastic deposit is partly formed of clasts and *in situ* small pahoehoe lobes, broken slabs of pahoehoe crust, which forms a palaeotopographic high. The upper invasive lava displays a vesicular nature, with distinct concentric amygdale bands. The lower lobe is formed of aphyric basalt, with little to no amygdales, and does not connect to parent lava within the cross-section of cliff, however, is assumed to connect in an area not exposed. (**d**) and (**e**) Schematic sketch of the invasive lava (**d**) and shallow intrusion (**e**).

with the surrounding compound lobes and it has thermally eroded into the underlying lobes, truncating them. The smaller tube *c.* 100 m to the south (Fig. 11a) has a diameter of 7.3 m and area of *c.* 47 m^2; the trend is uncertain because the tube is flush with the cliff. It presents concentric amygdales and fractures. Another tube, previously described as such by Kent *et al.* (1998), NE of Calgary Bay [NM 3685 5151] (Fig. 11b), has a diameter of *c.* 8.5 × 11.9 m, an area of *c.* 79.4 m^2 and a trend of 071°, which is a similar orientation to the larger Caliach Point tube. North of Caliach farm [NM 35616 53903], within the intertidal zone, a prominent partially eroded linear section of basalt is interpreted as another lava tube (Fig. 11c). It has a width of 1.5 m, extends *c.* 20 m into the sea and has a trend of 164°. Unlike the other tubes, this example is smaller and is found within the upper crust of a compound lobe >3 m thick, indicating that it may have initially formed as a lava channel.

Tumuli

Positive relief structures, known as tumuli, are common across modern and historical pahoehoe lava fields, although they are rarely documented within the geological record. Along the southern sea cliffs of Beinn Dull [NM 34377 46260], a localized palaeotopographic high, with a relative increase of 11 m, is observed where one lava appears to form a tumulus structure on its top surface (Fig. 12). Amygdaloidal

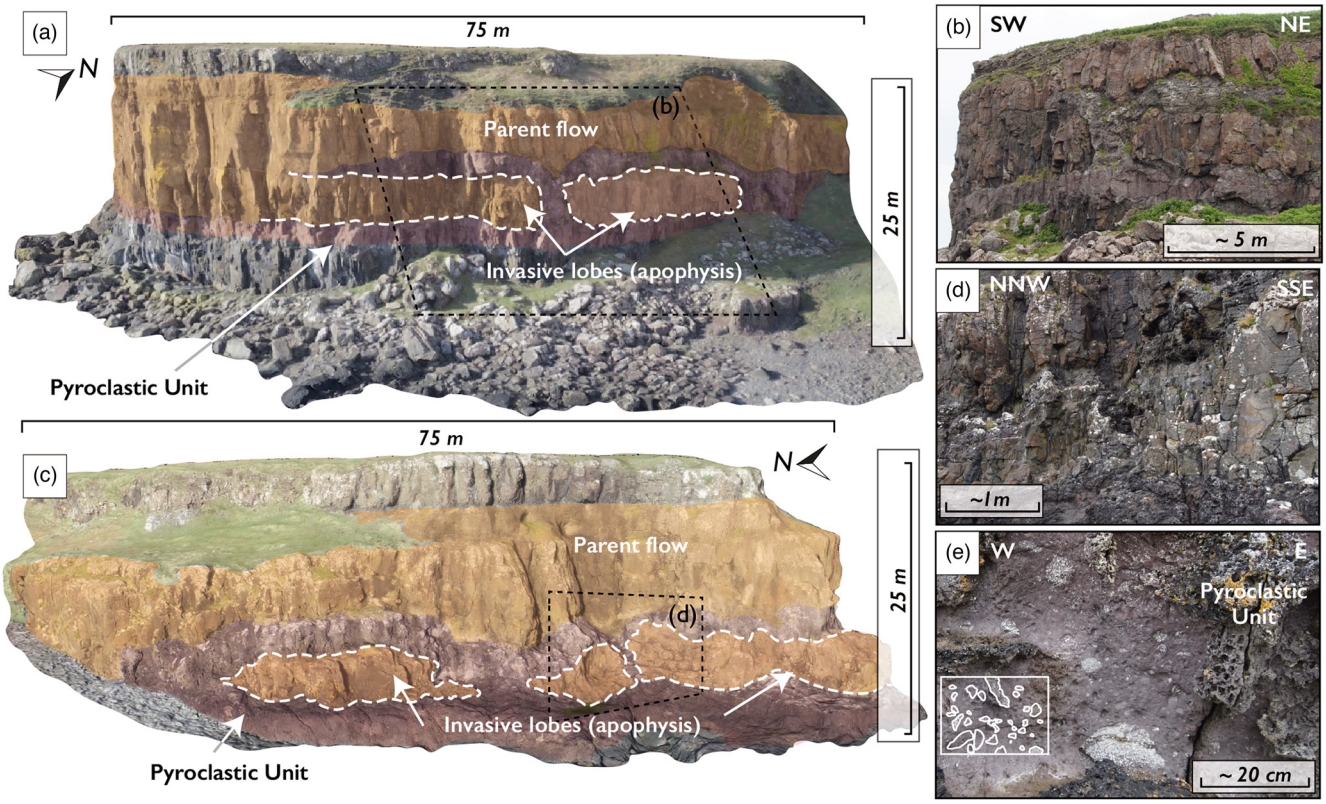

Fig. 10. Invasive (apophysis) lava. (**a**, **c**) Virtual outcrops displaying the same parent flow lobe with invasive lobes propagating into the volcaniclastic and slabby pahoehoe mounds below. (**b**) Field photograph of the same invasive lavas as in part (a), where a near-vertical column of volcaniclastic material propagates upwards and then laterally, separating the invasive flow lobes and the parent lava flow. (**d**) Field photograph of the same invasive lavas as in part (c), again with the poorly exposed volcaniclastic unit forming the substrate intruded by the invasive flow lobes. (**e**) Field photograph of smoothy eroded pyroclastic unit illustrating the clastic nature.

Downloaded from https://www.lyellcollection.org by Guest on Jul 10, 2025

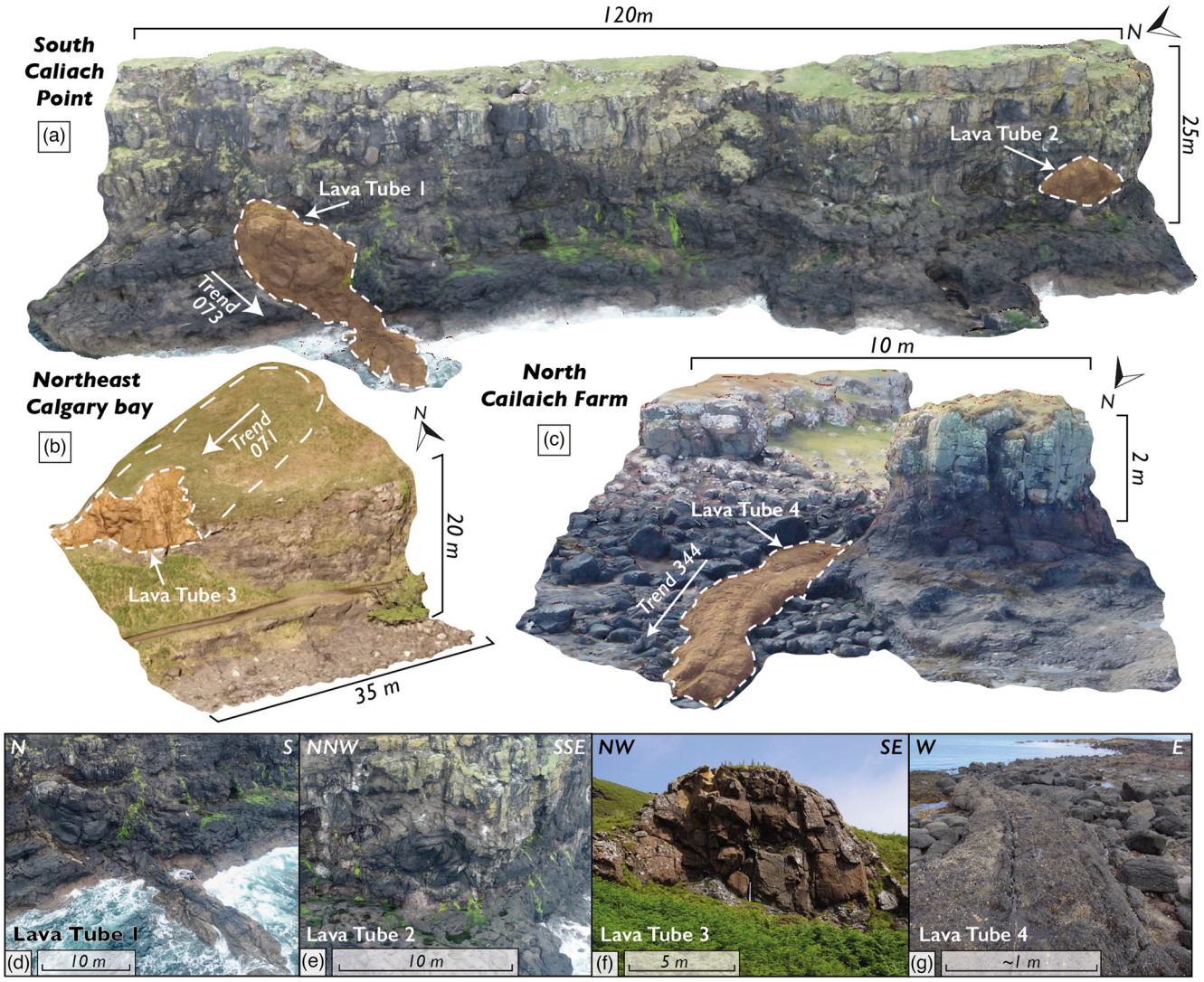

Fig. 11. Lava tubes across the Mull lava field. (**a**) Lava tubes found south of Caliach Point [NM 3480 5395]. Virtual outcrop of coastal cliffs where lava tubes 1 and 2 are both exposed. (**b**) Lava tube 3 at NE Calgary Bay [NM 3685 5151]. Virtual outcrop of the tube, with the oblique cross-section highlighted in orange and the linear raised mound assumed to be a continuation of the tube marked by the white dashed line. (**c**) Lava channel exposed north of Caliach Farm [NM 35616 53903]. Virtual outcrop of the lava channel and adjacent stack; the channel is within the vesicular upper crust of a lava, likely a flow within which the channel would have formed. (**d**–**g**) Field photos of the lava tubes 1–4.

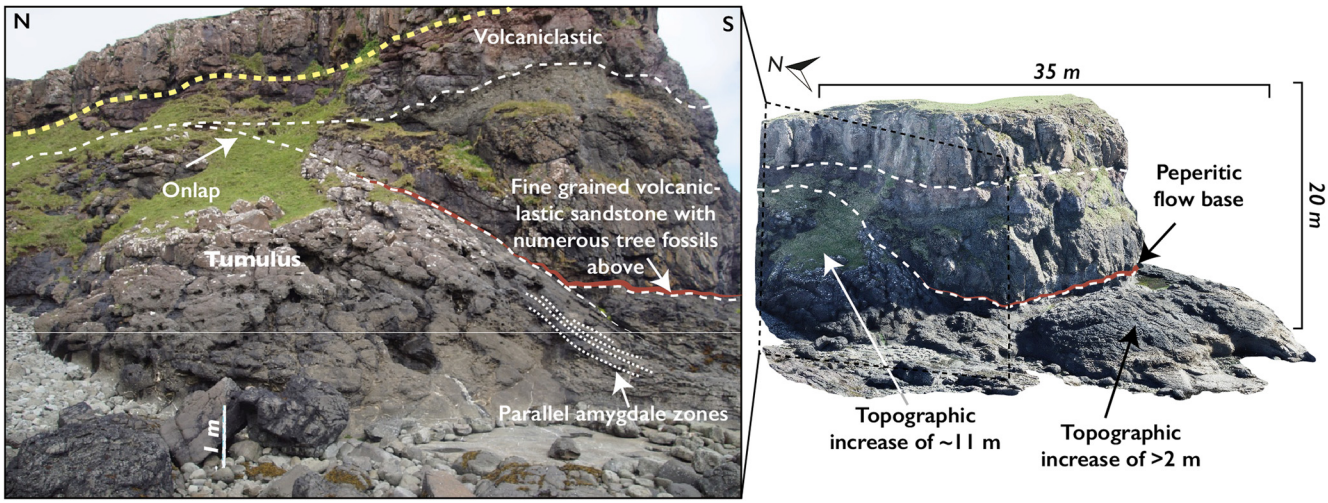

Fig. 12. Domed inflation structure interpreted as a tumulus [NM 34377 46260]. To the south, the overlying lavas onlap onto the structure. Within the tumulus, amygdale zones are present parallel to the top of dome, indicating little to no erosion between the tumulus and the onlapping lavas. The tumulus has a positive topography of *c.* 11 m and a slope of up to 37°. Amygdaloidal banding is seen in the top 2.5 m, along with irregular fractures that typically propagate along the axis of the tumulus.

Downloaded from https://www.lyellcollection.org by Guest on Jul 10, 2025

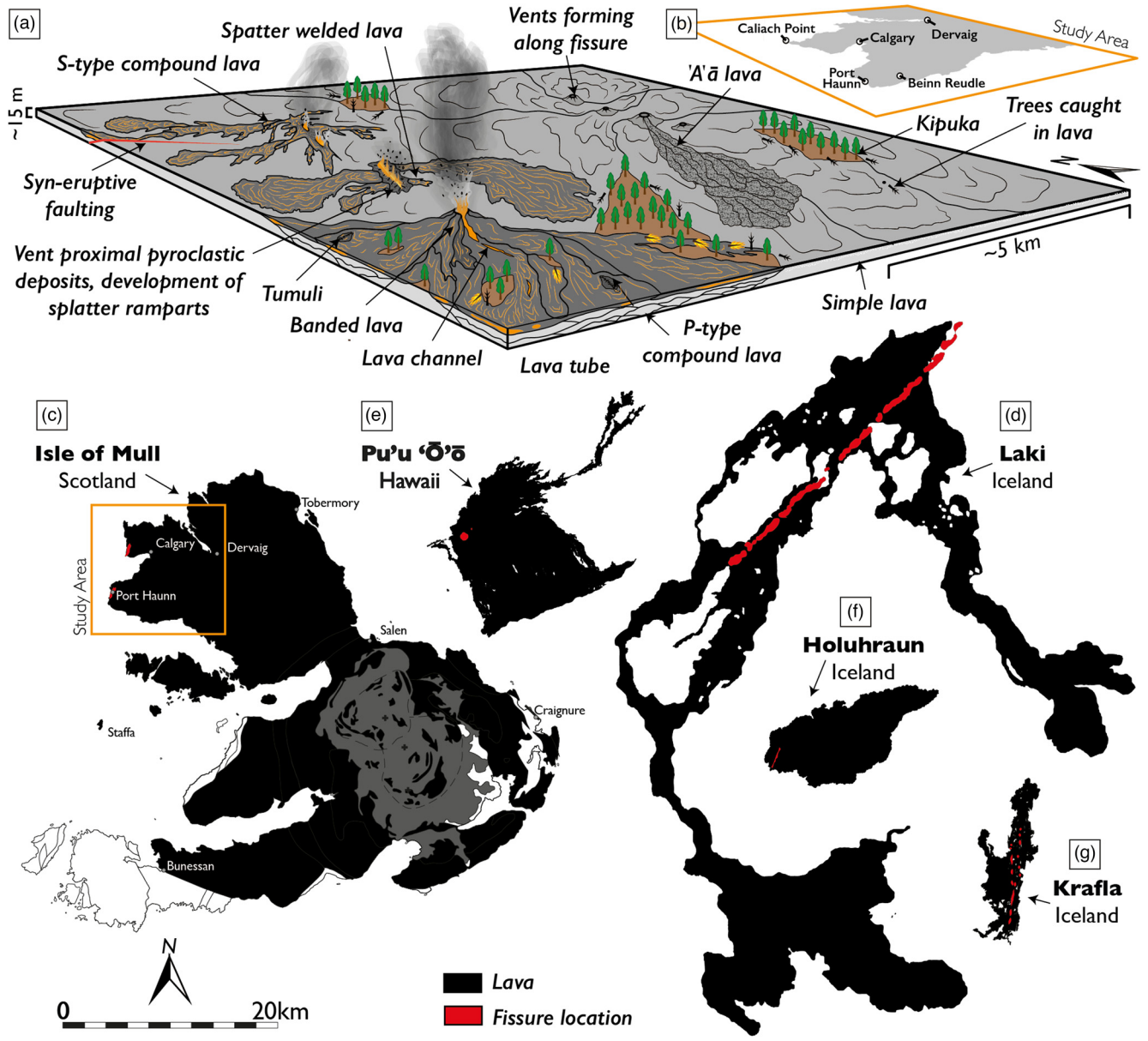

Fig. 13. Schematic block diagram reconstruction of the effusive environment and scale of NW Mull compared with the modern volcanic fields of Hawaii and Iceland. (**a**) Block diagram illustrating the lava plains volcanism of NW Mull; the diagram is generalized and does not represent an exact stratigraphic interval. (**b**) Location map of block diagram. (**c**) Isle of Mull, with 670 km^2 of lava and the associated intra-lava units mapped in black. Note that this represents all the exposures of hundreds to thousands of effusive events and that the lava stratigraphy of Mull has experienced significant erosion. (**d**) The Pu'u Ō'ō lava field, Hawaii, This is the longest recorded continuous effusive event (1983–2018). Outline adapted from. (**e**) The Laki (1783–84) lava field, Iceland. The vents formed along a large fissure with extensive sheet flows. (**f**) The Holuhraun (2014) lava field, Iceland. This is another fissure eruption that, through prolonged eruption effusion, focused along a main vent. (**g**) The Krafla (1975–84) lava field fissure within a graben-induced topographic low. Source: the lava field maps are traced from Google Earth, unless stated otherwise. The data provider for all locations is © Maxar Technologies. The outline of the lava field in part (e) is adapted from Thordarson and Self (1993).

bands form parallel to the tumuli edge at an angle of *c.* 35°. Two flow lobes, compound in nature, onlap the tumuli to the SE.

Discussion

The shallow intrusions, vent-proximal pyroclastic deposits and lava facies of NW Mull are interpreted in this study as direct evidence of a fissure-fed lava field, as illustrated in Figure 13a, b. The described deposits span multiple stratigraphic intervals, capturing the diversity of pyroclastic and effusive facies present within the stratigraphy. However, extensive faulting and exposure limitations prevent the correlation of individual eruptive events across the entire study area. Geologically young analogous fissure systems may offer insights into the lateral extent, duration and emplacement mechanisms of the Mull lava field (e.g. Fig. 13c–g).

Fissure systems of LIPs

LIPs represent the products of the largest known volcanic eruptions in Earth's history (Coffin and Eldholm 1994). During LIP development, batches of magma up to several thousand cubic kilometres in volume erupted onto the Earth's surface during individual eruptions, such as in the extensive lava flows of the Columbia River Basalt Province (Tolan *et al.* 2009; Reidel 2015) and the Deccan Traps (Self *et al.* 2008). Dykes, thought to represent the feeder pathways for these huge eruptions, are well documented in all LIPs, as are the resulting lava

Downloaded from https://www.lyellcollection.org by Guest on Jul 10, 2025

flows. However, few well-exposed examples exist of the transition between these subsurface domains and eruption sites.

Modern fissure systems

Some of the best exposures of geologically young fissure eruptions occur on modern day Hawaii and Iceland. Several parallels can be drawn between these geologically recent fissure deposits and the Mull lava field deposits described herein.

The Laki fissure eruption (1783–84) on Iceland is often used as an analogue for past LIP fissure eruptions due to its large lava volume (Thordarson and Self 1993). The Laki fissure system covers *c.* 599 km^2 (Fig. 13d) and produced lava over seven months, emplacing flows onto irregular topography and into a glacial drainage system, resulting in localized lava ponding and channelling (Thordarson and Self 1993). It consists of a 4–28 m wide feeder dyke, vent-proximal pyroclastic deposits and an extensive lava flow field (Thordarson and Self 1993; Reynolds *et al.* 2016). The pyroclastic deposits include fluidal lapilli, spatter bombs that agglutinate, fractured scoria bombs, and armoured lapilli and bombs, with units <0.5–6 m thick (Reynolds *et al.* 2016). Welded deposits (e.g. agglutinated spatter) are predominantly present close to the dyke-filled fissure. Similar vent-proximal deposit associations in the Mull lava field, albeit on a smaller scale, appear comparable in terms of eruption styles. The lava flows produced from the Laki fissure are described as 2–20 m thick columnar-jointed pahoehoe, clastogenic pahoehoe, lava-like agglutinate and shelly pahoehoe (Reynolds *et al.* 2016), again similar to the range found in the study area on Mull.

The Hawaiin Pu'u 'Ō'ō fissure eruption (1983–2018) was a prolonged effusive event, generating a 144 km^2 (Fig. 13e) lava field (Patrick *et al.* 2020). As a result of Hawaii's ocean island setting, lava flowed into the ocean, forming hyaloclastite and pillow lavas. The subaerial field consists predominantly of pahoehoe lava with localized 'a'ā flows (Self *et al.* 1998). Pahoehoe lobes range from 0.2 to 0.3 m thick pre-inflation and to 1–5 m post-inflation (Hon *et al.* 1994), with both S- and P-type pahoehoe present (Wilmoth and Walker 1993). These characteristics are analogous to the compound pahoehoe lobes of the Mull lava field, indicating a similar emplacement style. However, the Pu'u 'Ō'ō lava field developed on a significantly steeper slope than that inferred for the Mull lava field.

The Holuhraun fissure eruption (2014–2015) on Iceland produced an 84.2 km^2 lava field (Fig. 13f) over relatively flat terrain, with individual flows reaching 1–6 m in thickness before inflation (Kolzenburg *et al.* 2017; Dirscherl and Rossi 2018; Tarquini *et al.* 2018). The longest flow (17 km) developed early in the eruption (Pedersen *et al.* 2017), with later stage flows influenced by lava channels and tubes. The presence of lava tubes, channels and tumuli on a relatively flat palaeotopography in the Mull lava field suggests a comparable style of lava transport and inflation-driven emplacement.

The Krafla fissure eruptions (1975–1984) on Iceland generated an 84.2 km^2 lava field (Fig. 13g) within a graben (Rossi 1997). With an average thickness of 11 m, the initial 2 m lobes inflated up to 26 m. Syn-eruptive faulting influenced lava ponding and inflation, a process also inferred for the Mull lava field case study. Krafla provides a model for fault-controlled lava distribution, analogous to some of the thickest simple flows in the Mull lava field potentially resulting from fault-induced ponding.

Vent-proximal pyroclastic deposits

The localities of Port Haunn and Calgary Bay on Mull present extensive pyroclastic deposits with numerous characteristics associated with vent-proximal deposits of Hawaiian-style eruptive activity. The lack of continuous exposure between these localities prevents documentation of the continuity of the deposits; however, the similarity and equivalent stratigraphic position is conformable with similar spatio-temporal processes, even if not connected by a continuous fissure system.

The pyroclasts consist of primary tuff, scoria, blocks and bombs, as well as spatter-welded lavas. Significant variations in pyroclast size and the extent of welding throughout the deposit indicate pulsing in the fissure fountain and changes in the accumulation rate (e.g. Wolfe *et al.* 1988; Valentine and Groves 1996; Valentine and Gregg 2008; Reynolds *et al.* 2016). Evidence of non-welded scoria lapilli suggests lava fountaining, potentially to a significant height (e.g. 100 m), because the clasts are of a similar size and shape to those described by Reynolds *et al.* (2016) at Laki. Spatter-welded lava (e.g. those underlying and intercalated with the banded lavas) may be indicative of periods of decreased fountain height, resulting in larger clasts (Head and Wilson 1989) that cooled more slowly, leading to welding and agglutination (Sumner *et al.* 2005; Reynolds *et al.* 2016).

Although most of the deposit appears conformable with the primary pyroclastic deposition, there is evidence of localized reworking, such as clearly rounded clasts and imbrication a few kilometres from the areas described. The pyroclastic deposits and associated lavas are subaerial deposits and, given the abundance of tree fossils (moulds, casts and mineralogically replaced remnants) around this stratigraphic interval, it is likely that localized reworking occurred. This is observed elsewhere (e.g. Iceland) where areas of pyroclastic deposits not covered by later effusion are easily eroded and provide sediment to drainage systems, forming volcaniclastic deposits (e.g. Lacasse *et al.* 1998). Pyroclastic eruptions are well known to actively form lahars and debris flow deposits, often resulting in a large input of volcanic material into drainage systems (Vallance and Iverson 2015).

Intrusive fissure deposits

Fissure eruptions are fed through a network of intrusions; however, exposures of the transition from intrusion to surface eruption are rare due to the localized and dynamic nature of the transition zone. The pyroclastic deposits of Port Haunn and NW Calgary Bay are intruded by multiple ragged dykes and irregular intrusions. These intrusions terminate below the top of the pyroclastic deposits and are interpreted as a complex network of partially drained feeder dykes.

At Port Haunn, the 35 m high section of aphanitic prismatic basalt is potentially the remnants of a vent structure, possibly formed as part of the same fissure system through prolonged effusion, either as an infilled crater or a small lava lake. An alternative interpretation is that it was formed as locally ponded lava. The partial exposure hampers the identification of the exact emplacement method, so both options are considered viable. The numerous shallow intrusions, dykes and plugs are also likely to be part of this fissure plumbing system.

The NW Calgary exposure reveals several dykes of varying orientations: the NW–SE regional trend and the NE–SW trend of the partially drained dykes. Dykes and fissures typically harness weaknesses in the country rock and, although the NW–SE trend is dominant regionally, there are several faults documented in this area (Fig. 1a) that also follow the NE–SW trend. Therefore, although previous workers prefer the NW–SE trend for expected fissures, it appears plausible that fissures formed along both the NW–SE and NE–SW trends.

Effusive fissure deposits

A wide range of effusive deposits are documented across the study area of NW Mull, with exposures dominated by subaerial lava flows of various types, which is in agreement with the general

Downloaded from https://www.lyellcollection.org by Guest on Jul 10, 2025

observations from previous studies in and around the study area (Bailey *et al.* 1924; Williamson and Bell 2012; Hole *et al.* 2023). This study documents simple tabular and compound lava flows, with the flow characteristics dominated by pahoehoe lava flow features (including both P-type and S-type), but also locally representing transitional through to ʻaʻā flow types (Peterson and Tilling 1980; Self *et al.* 1996; Thordarson and Self 1998; Jerram *et al.* 2002; Passey and Bell 2007). It has been inferred that the lava flows of NW Mull were fissure-fed; however, only limited evidence for the fissure eruption sites of these flows has been identified to date (Williamson and Bell 2012). The majority of the subaerial lava flow facies documented within this study do not give unambiguous evidence for proximity to an eruption source. However, certain important observations do give supporting evidence for close fissure proximity.

In several locations, including at [NM 3494 5294], compound lava sequences dominated by small and thin S-type pahoehoe compound toe lobes are observed. Very high porosity (weakly degassed) spongy pahoehoe flows are generally accepted to be a feature of vent-proximal lava flows that have solidified prior to significant transport, which would enable more efficient degassing (Wilmoth and Walker 1993). These small and discontinuous S-type compound lobes occur in close association with examples of spatter-welded lava and associated pyroclastic deposits. Together with this association of facies, the S-type lavas give support for fissure vent-proximal eruptions interpreted here as part of a contiguous fissure eruption series deposited in the vicinity of the active fissure.

P-type pahoehoe is also common and is often associated with tube-fed volcanism (Wilmoth and Walker 1993). Therefore, given the superposition of these facies with the S-type lavas, these deposits may represent relatively more source-distal flows, implying that the fissure locations within the study area were not fixed throughout the eruption sequence, a feature common to modern fissure-fed rift systems, such as Iceland (Einarsson *et al.* 2023). It should also be noted that fissure vent-proximal tube systems are well documented from various settings (Wantim *et al.* 2011; Belousov *et al.* 2015; Pedersen *et al.* 2017) and therefore the presence of tubes is not inconsistent with a fissure vent-proximal location.

Several lava tubes are identified within the study area (Fig. 11). Lava tubes are known to have a fundamental role in the propagation of lava fields away from fissures (Greeley 1987; Hon *et al.* 1994; Peterson *et al.* 1994). The lava tubes vary in size and orientation, with the largest examples (lava tubes 1 and 3) potentially comprising longer lived W–NW-oriented master tube feeders due to their larger size and, in the case of lava tube 1, down-cutting features (Greeley 1987). Smaller examples, such as lava tube 2, likely represent more local distributary tubes. Lava tube 4, with its amygdaloidal, rough-textured top surface and small sinuous shape, shows the attributes of a shallow lava tube. Given that this tube appears to occur within *c.* 2 m of the flow's upper crust, it is plausible that this tube originated as a lava channel and developed into a lava tube, a process described in many modern lava fields (e.g. Greeley 1987; Cas and Wright 1991; Wilmoth and Walker 1993; Calvari and Pinkerton 1998).

Implications of the NW Mull fissure zone

The NW region of the Paleogene Mull lava field formed through a series of fissures dominated by Hawaiian-style basaltic volcanism. This study provides evidence supporting the long-standing theory that the BPIP lava fields formed through fissure eruptions, first proposed by Geike (1871) and widely adopted in more recent studies (Williamson and Bell 2012; Jolley *et al.* 2023). Figure 13a presents a schematic synthesis of the proposed Mull fissure system, highlighting the anticipated eruption environment. Dykes propagating NE–SW harnessed pre-existing lines of weakness following the Caledonian orogenic fabric to reach the surface, forming fire fountains and build-ups of vent-proximal basaltic eruptive sequences. It is plausible that other fissures exploited the NW–SE-trending regional dyke swarm, forming a conjugate system, given the inherited structural complexity, as indicated by the fault orientations in Figure 1a. Jolly and Sanderson (1995) demonstrated that, although the majority (55%) of the Mull dyke swarm intrusions align with the dominant NW–SE trend, certain dykes deviate, exhibiting oblique orientations relative to the primary swarm.

The emplacement timing of these diverted dykes remains poorly constrained and their genetic relationship to the surrounding lava sequences is debated (Ishizuka *et al.* 2017). MacDonald *et al.* (2010) proposed that these dykes share their geochemistry with the plateau lavas, whereas Kerr *et al.* (1999) suggest an association with the Central Mull Tholeiites, with occasional occurrences of Coire Gorm type compositions. Nevertheless, the NE–SW-propagating fissures of NW Mull produced airfall basaltic tephra and vent-proximal spatter, locally forming spatter rampart structures, alongside feeding effusive lavas that began to build up the developing lava field, commonly fed by a network of lava tubes. In several cases, evidence for spatter-welded lavas are seen, which likely formed on the flanks of the fissure deposits.

Lava flows fed from the fissure system range from vent-proximal banded and S-type pahoehoe flows through to tube-fed P-type pahoehoe compound lobes and less common examples of ʻaʻā and invasive lava flows. Prolonged eruption formed spatter ramparts on a smaller scale than those developed during the Laki eruption (Thordarson and Self 1993), alongside the development of thicker, more laterally extensive and inflated simple lava flows fed by lava tubes. Extensive tree fossils (moulds, casts and mineralogically replaced remnants), like those described by Bell and Williamson (2017) and Pugsley (2021), represent either local (kipuka) or potentially regional volcanic hiatuses throughout the NW Mull lava sequence. This study documents evidence for the eruption of the NAIP sequence in this area by processes commonly observed in modern basaltic fissure systems and on a scale well within those documented from, for example, Laki (Thordarson and Self 1993; Self *et al.* 1998; Reynolds *et al.* 2016).

Conclusions

Through the integration of traditional field mapping with modern, high-resolution photogrammetry, this study documents a remarkably well-preserved example of a dissected dyke-fed fissure zone within the NAIP LIP. The following conclusions can be drawn from this study.

(1) Basaltic fissure-fed Hawaiian-style volcanism formed the NW Mull lava field, as indicated by dissected feeder dykes, vent-proximal pyroclastic deposits and the associated effusive lava facies.
(2) The NE–SW-oriented fissures likely harnessed structural features inherited from the Caledonian Orogeny rather than aligning with the regional dyke swarm.
(3) The NW Mull lava field presents a heterogeneous sequence of lavas and inter-lava pyroclastic and volcaniclastic units. It exhibits significant structural complexity, which juxtaposes numerous sections of stratigraphy together along the coast.
(4) The area exhibits a classic plains volcanism habit, which is largely pahoehoe in nature, with fissure-fed volcanism developing lava channels, lava tube feeder networks and tumuli.
(5) The outcrop exposures of coastal NW Mull support the long-standing theory that many of the lavas of the BPIP were fed by fissures.

Downloaded from https://www.lyellcollection.org by Guest on Jul 10, 2025

Scientific editing by Renjie Zhou

Acknowledgements We thank the locals of Mull, with particular emphasis to those to whose land covers the study area (including Shirley and Bob Strachan; Carolyne and Somerset Charrington, Willie and the late Ann MacPhail). They were so often welcoming and interested in how a geologist sees their home. We also thank Kenny Turnbull and Colin Morrison for our view of the cliffs from the sea. We thank the anonymous reviewer and Editor Renjie Zhou for their time and help in improving this paper.

Author contributions **JHP**: conceptualization (equal), data curation (lead), formal analysis (equal), funding acquisition (equal), investigation (lead), methodology (equal), visualization (equal), writing – original draft (lead), writing – review and editing (equal); **MJH**: conceptualization (equal), funding acquisition (equal), project administration (lead), supervision (lead), visualization (equal), writing – review and editing (equal); **DWJ**: conceptualization (supporting), supervision (equal), visualization (equal), writing – review and editing (equal); **JMM**: conceptualization (equal), methodology (equal), supervision (equal), visualization (equal), writing – original draft (equal), writing – review and editing (equal); **JAH**: data curation (equal), funding acquisition (equal), methodology (equal), software (lead), supervision (equal), visualization (supporting), writing – original draft (supporting), writing – review and editing (equal); **AH**: conceptualization (supporting), methodology (supporting), writing – original draft (equal), writing – review & editing (supporting); **AKQ**: conceptualization (equal), data curation (supporting), writing – original draft (equal), writing – review and editing (supporting); **JW**: data curation (supporting), investigation (supporting), methodology (supporting), writing – original draft (supporting), writing – review & editing (supporting); **NF**: data curation (supporting), investigation (supporting), writing – original draft (supporting).

Funding This work was funded through several sources, including internal University of Aberdeen scholarships and bursaries, in additional fieldwork-specific funding from the Cambridge Arctic Shelf Programme (part funded fieldwork through the 2017 Fieldwork Grant). The processing of the virtual outcrop was funded through SafariDB (Sedimentary Architecture of Field Analogues for Reservoir Information Database, part funded collection and processing of virtual outcrop).

Competing interests The authors declare that they have no known competing financial interests or personal relationships that could have appeared to influence the work reported in this paper.

Data availability The datasets generated during and/or analysed during the current study are available in the v3geo repository, https://v3geo.com

References

Archer, S.G., Bergman, S.C., Iliffe, J., Murphy, C.M. and Thornton, M. 2005. Palaeogene igneous rocks reveal new insights into the geodynamic evolution and petroleum potential of the Rockall Trough, NE Atlantic Margin. *Basin Research*, **17**, 171–201, https://doi.org/10.1111/j.1365-2117.2005.00260.x

Bell, B.R. and Williamson, I.T. 2017. Fossil trees, tree moulds and tree casts in the Palaeocene Mull Lava Field, NW Scotland: context, formation and implications for lava emplacement. *Earth and Environmental Science Transactions of the Royal Society of Edinburgh*, **107**, 53–71, https://doi.org/10.1017/S175569101700007X

Bailey, E.B., Clough, C.T., Wright, W.B., Richey, J.E. and Wilson, G.V. 1924. *The Tertiary and Post-Tertiary Geology of Mull, Loch Aline and Oban*. Geological Survey of Great Britain, Memoirs.

Belousov, A., Belousova, M., Edwards, B., Volynets, A. and Melnikov, D. 2015. Overview of the precursors and dynamics of the 2012–13 basaltic fissure eruption of Tolbachik Volcano, Kamchatka, Russia. *Journal of Volcanology and Geothermal Research*, **307**, 22–37, https://doi.org/10.1016/j.jvolgeores.2015.06.013

Black, B., Mittal, T., Lingo, F., Walowski, K. and Hernandez, A. 2021. Assessing the environmental consequences of the generation and alteration of mafic volcaniclastic deposits during large igneous province emplacement. *In*: Ernst, R.E., Dickerson, A.J. and Bekker, A. (eds), *Large Igneous Provinces: A Driver of Global Environmental and Biotic Changes*. Wiley, 117–131.

Brown, D.J. and Bell, B.R. 2007. Debris flow deposits within the Palaeogene lava fields of NW Scotland: evidence for mass wasting of the volcanic landscape during emplacement of the Ardnamurchan Central Complex. *Bulletin of Volcanology*, **69**, 847–868, https://doi.org/10.1007/s00445-007-0114-9

Brown, R.J., Thordarson, T., Self, S. and Blake, S. 2015. Disruption of tephra fall deposits caused by lava flows during basaltic eruptions. *Bulletin of Volcanology*, **77**, 1–15, https://doi.org/10.1007/s00445-015-0974-3

Buckley, S.J., Howell, J.A., Enge, H.D. and Kurz, T.H. 2008. Terrestrial laser scanning in geology: data acquisition, processing and accuracy considerations. *Journal of the Geological Society, London*, **165**, 625–638, https://doi.org/10.1144/0016-76492007-100

Buckley, S.J., Ringdal, K., Naumann, N., Dolva, B., Kurz, T.H., Howell, J.A. and Dewez, T.J. 2019. LIME: software for 3-D visualization, interpretation, and communication of virtual geoscience models. *Geosphere*, **15**, 222–235, https://doi.org/10.1130/GES02002.1

Buckley, S.J., Howell, J.A. *et al.* 2021. V3Geo: a cloud-based repository for virtual 3D models in geoscience. *Geoscience Communication Discussions*, **2021**, 1–27, https://doi.org/10.5194/gc-5-67-2022

Büyükakpınar, P., Isken, M.P. *et al.* 2025. Understanding the seismic signature of transtensional opening in the Reykjanes Peninsula rift zone, SW Iceland. *Journal of Geophysical Research: Solid Earth*, **130**, e2024JB029566, https://doi.org/10.1029/2024JB029566

Byerly, G. and Swanson, D.A. 1978. Invasive Columbia River basalt flows along the northwestern margin of the Columbia Plateau, north-central Washington. *GSA, Abstracts with Programs*, **10**, 98.

Calvari, S. and Pinkerton, H. 1998. Formation of lava tubes and extensive flow field during the 1991–1993 eruption of Mount Etna. *Journal of Geophysical Research: Solid Earth*, **103**, 27291–27301.

Carey, S. and Sparks, R.S.J. 1986. Quantitative models of the fallout and dispersal of tephra from volcanic eruption columns. *Bulletin of Volcanology*, **48**, 109–125.

Cas, R.A. and Wright, J.V. 1991. Subaqueous pyroclastic flows and ignimbrites: an assessment. *Bulletin of Volcanology*, **53**, 357–380.

Coffin, M.F. and Eldholm, O. 1994. Large igneous provinces: crustal structure, dimensions, and external consequences. *Reviews of Geophysics*, **32**, 1–36, https://doi.org/10.1029/93RG02508

Dirscherl, M. and Rossi, C. 2018. Geomorphometric analysis of the 2014–2015 Bárðarbunga volcanic eruption, Iceland. *Remote Sensing of Environment*, **204**, 244–259, https://doi.org/10.1016/j.rse.2017.10.027

Einarsson, P., Eyjólfsson, V. and Hjartardóttir, Á.R. 2023. Tectonic framework and fault structures in the Fagradalsfjall segment of the Reykjanes Peninsula oblique rift, Iceland. *Bulletin of Volcanology*, **85**, 9, https://doi.org/10.1007/s00445-022-01624-x

Emeleus, C.H. and Bell, B.R. 2005. *British Regional Geology: the Palaeogene Volcanic Districts of Scotland*. 4th edn. British Geological Survey, Nottingham.

Famelli, N., Millett, J.M. *et al.* 2021. Characterizing the nature and importance of lava–sediment interactions with the aid of field outcrop analogues. *Journal of South American Earth Sciences*, **108**, 103–108, https://doi.org/10.1016/j.jsames.2020.103108

Fisher, R.V. 1961. Proposed classification of volcaniclastic sediments and rocks. *Geological Society of America Bulletin*, **72**, 1409–1414.

Fisher, R.V. and Schmincke, H.U. 1984. *Pyroclastic Rocks and Tectonic Environment*. Springer, Berlin, 383–409.

Fyfe, L.J.C., Schofield, N., Holford, S., Hartley, A., Heafford, A., Muirhead, D. and Howell, J. 2021. Geology and petroleum prospectivity of the Sea of Hebrides Basin and Minch Basin, offshore NW Scotland. *Petroleum Geoscience*, **27**, https://doi.org/10.1144/petgeo2021-003

Garcia, M.O., Pietruszka, A.J., Norman, M.D. and Rhodes, J.M. 2021. Kīlauea's Pu'u 'Ō'ō eruption (1983–2018): a synthesis of magmatic processes during a prolonged basaltic event. *Chemical Geology*, **581**, 120391, https://doi.org/10.1016/j.chemgeo.2021.120391

Geike, A. 1871. On the Tertiary igneous rocks of the British Isles. *Quarterly Journal of the Geological Society of London*, **27**, 279–311, https://doi.org/10.1144/GSL.JGS.1871.027.01-02.40

Geike, A. 1894. On the relations of the basic and acid rocks of the Tertiary volcanic series of the Inner Hebrides. *Quarterly Journal of the Geological Society of London*, **50**, 212–231, https://doi.org/10.1144/GSL.JGS.1894.050.01-04.18

Gillespie, M. and Styles, M. 1999. *BGS Rock Classification Scheme, Volume 1. Classification of Igneous Rocks*. British Geological Survey.

Greeley, R. 1987. The role of lava tubes in Hawaiian volcanoes. *US Geological Survey, Professional Papers*, **1350**, 1589–1602.

Haliday, A.N., Aftalion, M., Van Breemen, O. and Jocelyn, J. 1979. Petrogenetic significance of Rb–Sr and U–Pb isotopic systems in the 400 Ma old British Isles granitoids and their hosts. *Geological Society, London, Special Publications*, **8**, 653–661, https://doi.org/10.1144/GSL.SP.1979.008.01.79

Head, J.W. and Wilson, L. 1989. Basaltic pyroclastic eruptions: influence of gas-release patterns and volume fluxes on fountain structure, and the formation of cinder cones, spatter cones, rootless flows, lava ponds and lava flows. *Journal of Volcanology and Geothermal Research*, **37**, 261–271, https://doi.org/10.1016/0377-0273(89)90083-8

Hesselbo, S.P., Oates, M.J. and Jenkyns, H.C. 1998. The lower Lias Group of the Hebrides Basin. *Scottish Journal of Geology*, **34**, 23–60, https://doi.org/10.1144/sjg34010023

Holdsworth, R.E., Harris, A.L. and Roberts, A.M. 1987. The stratigraphy, structure and regional significance if the Moine Rocks of Mull, Argyllshire, W. Scotland. *Geological Journal*, **22**, 83–107, https://doi.org/10.1002/gj.3350220203

Hole, M.J., Millett, J.M., Rogers, N.W. and Jolley, D.W. 2015. Rifting and mafic magmatism in the Hebridean basins. *Journal of the Geological Society*, **172**, 218–236, https://doi.org/10.1144/jgs2014-100

Hole, M.J., Pugsley, J.H., Jolley, D.W. and Millett, J.M. 2023. Fractional crystallization of garnet in alkali basalts at >1.8 GPa and implications for geochemical diversity of Large Igneous Provinces. *Lithos*, **460**, 107397, https://doi.org/10.1016/j.lithos.2023.107397

Downloaded from https://www.lyellcollection.org by Guest on Jul 10, 2025

Holm, R.F. 1987. Significance of agglutinate mounds on lava flows associated with monogenetic cones: an example at Sunset Crater, northern Arizona. *Geological Society of America Bulletin*, **99**, 319–324.

Hon, K., Kauahikaua, J., Denlinger, R. and Mackay, K. 1994. Emplacement and inflation of pahoehoe sheet flows: observations and measurements of active lava flows on Kilauea Volcano, Hawaii. *Geological Society of America Bulletin*, **106**, 351–370.

Hooper, P. 1997. The Columbia River flood basalt province: current status. *American Geophysical Union, Geophysical Monograph Series*, **100**, 1–27, https://doi.org/10.1029/GM100p0001

Houghton, B.F., Bonadonna, C., Gregg, C.E., Johnston, D.M., Cousins, W.J., Cole, J.W. and Del Carlo, P. 2006. Proximal tephra hazards: recent eruption studies applied to volcanic risk in the Auckland volcanic field, New Zealand. *Journal of Volcanology and Geothermal Research*, **155**, 138–149, https://doi.org/10.1016/j.jvolgeores.2006.02.006

Howell, J., Chmielewska, M., Lewis, C., Buckley, S., Naumann, N. and Pugsley, J. 2021. Acquisition of data for building photogrammetric virtual outcrop models for the geosciences using remotely piloted vehicles (RPVs), https://doi.org/10.31223/X54914

Ishizuka, O., Taylor, R.N., Geshi, N. and Mochizuki, N. 2017. Large-volume lateral magma transport from the Mull volcano: an insight to magma chamber processes. *Geochemistry, Geophysics, Geosystems*, **18**, 1618–1640, https://doi.org/10.1002/2016GC006712

Jacques, J.M. and Reavy, R.J. 1994. Caledonian plutonism and major lineaments in the SW Scottish Highlands. *Journal of the Geological Society, London*, **151**, 955–969, https://doi.org/10.1144/gsjgs.151.6.0955

Jerram, D.A., Menzies, M.A., Klemperer, S.L., Ebinger, C.J. and Baker, J. 2002. Volcanology and facies architecture of flood basalts. *GSA, Special Papers*, **362**, 119–132, https://doi.org/10.1130/0-8137-2362-0.119

Jolley, D.W., Millett, J., Malcolm, H.O.L.E. and Pugsley, J. 2023. Integrated photogrammetry, lava geochemistry and palynological re-evaluation of the early evolution of the topographically constrained Mull lava field, Scotland. *Earth and Environmental Science Transactions of the Royal Society of Edinburgh*, **114**, 193–217, https://doi.org/10.1017/S1755691023000191

Jolly, R.J.H. and Sanderson, D.J. 1995. Variation in the form and distribution of dykes in the Mull swarm, Scotland. *Journal of Structural Geology*, **17**, 1543–1557, https://doi.org/10.1016/0191-8141(95)00046-G

Judd, J.W. 1886. On the gabbros, dolerites, and basalts, of Tertiary age, in Scotland and Ireland. *Quarterly Journal of the Geological Society of London*, **42**, 49–95, https://doi.org/10.1144/GSL.JGS.1886.042.01-04.13

Judd, J.W. 1889. The Tertiary volcanoes of the Western Isles of Scotland. *Quarterly Journal of the Geological Society of London*, **45**, 187–218, https://doi.org/10.1144/GSL.JGS.1889.045.01-04.14

Kehl, C., Buckley, S.J., Gawthorpe, R.L., Viola, I. and Howell, J.A. 2016. Direct image-to-geometry registration using mobile sensor data. *ISPRS Annals of the Photogrammetry, Remote Sensing and Spatial Information Sciences*, **3**, 121–128, https://doi.org/10.5194/isprs-annals-III-2-121-2016

Kent, R.W. and Fitton, J.G. 2000. Mantle sources and melting dynamics in the British Palaeogene Igneous Province. *Journal of Petrology*, **41**, 1023–1040, https://doi.org/10.1093/petrology/41.7.1023

Kent, R.W., Thomson, B.A., Skelhorn, R.R., Kerr, A.C., Norry, M.J. and Walsh, J.N. 1998. Emplacement of Hebridean Tertiary flood basalts: evidence from an inflated pahoehoe lava flow on Mull, Scotland. *Journal of the Geological Society, London*, **155**, 599–607, https://doi.org/10.1144/gsjgs.155.4.0599

Kerr, A.C. 1993. *The Geochemistry and Petrogenesis of the Mull and Morvern Tertiary Lava Succession, Argyll, Scotland*. PhD thesis, Durham University.

Kerr, A.C. 1995. The geochemistry of the Mull–Morvern Tertiary lava succession, NW Scotland: an assessment of mantle sources during plume-related volcanism. *Chemical Geology*, **122**, 43–58, https://doi.org/10.1016/0009-2541(95)00009-B

Kerr, A.C. 1997. The geochemistry and significance of plugs intruding the Tertiary Mull–Morvern lava succession, western Scotland. *Scottish Journal of Geology*, **33**, 157–167, https://doi.org/10.1144/sjg33020157

Kerr, A.C., Kempton, P.D. and Thompson, R.N. 1995. Crustal assimilation during turbulent magma ascent (ATA); new isotopic evidence from the Mull Tertiary lava succession, NW Scotland. *Contributions to Mineralogy and Petrology*, **119**, 142–154, https://doi.org/10.1007/s004100050032

Kerr, A.C., Kent, R.W., Thomson, B.A., Seedhouse, J.K. and Donaldson, C.H. 1999. Geochemical evolution of the Tertiary Mull volcano, western Scotland. *Journal of Petrology*, **40**, 873–908, https://doi.org/10.1093/petroj/40.6.873

Kolzenburg, S., Giordano, D., Thordarson, T., Höskuldsson, A. and Dingwell, D.B. 2017. The rheological evolution of the 2014/2015 eruption at Holuhraun, central Iceland. *Bulletin of Volcanology*, **79**, 1–16, https://doi.org/10.1007/s00445-017-1128-6

Lacasse, C., Carey, S. and Sigurdsson, H. 1998. Volcanogenic sedimentation in the Iceland Basin: influence of subaerial and subglacial eruptions. *Journal of Volcanology and Geothermal Research*, **83**, 47–73, https://doi.org/10.1016/S0377-0273(98)00015-8

MacDonald, G.A. 1972. Composite lava flows on Haleakala Volcano, Hawaii. *Geological Society of America Bulletin*, **83**, 2971–2974.

MacDonald, R., Baginski, B., Upton, B.G.J., Pinkerton, H., MacInnes, D.A. and MacGillivray, J.C. 2010. The Mull Palaeogene dyke swarm: insights into the evolution of the Mull igneous centre and dyke-emplacement mechanisms. *Mineralogical Magazine*, **74**, 601–622, https://doi.org/10.1180/minmag.2010.074.4.601

MacDonald, R., Fettes, D.J. and Bagiński, B. 2015. The Mull Paleocene dykes: some insights into the nature of major dyke swarms. *Scottish Journal of Geology*, **51**, 116–124, https://doi.org/10.1144/sjg2014-016

Mège, D. and Korme, T. 2004. Fissure eruption of flood basalts from statistical analysis of dyke fracture length. *Journal of Volcanology and Geothermal Research*, **131**, 77–92, https://doi.org/10.1016/S0377-0273(03)00317-2

Mihalffy, P., Steinberger, B. and Schmeling, H. 2008. The effect of the large-scale mantle flow field on the Iceland hotspot track. *Tectonophysics*, **447**, 5–18, https://doi.org/10.1016/j.tecto.2006.12.012

Millett, J.M., Hole, M.J., Jolley, D.W., Schofield, N. and Campbell, E. 2016. Frontier exploration and the North Atlantic Igneous Province: new insights from a 2.6 km offshore volcanic sequence in the NE Faroe–Shetland Basin. *Journal of the Geological Society*, **173**, 320–336, https://doi.org/10.1144/jgs2015-069

Millett, J.M., Jolley, D.W., Hole, M.J., Augland, L., Pugsley, J.H., McLeod, G.W. and Planke, S. 2024. High-precision U–Pb zircon dating of explosive volcanism in an early bi-modal volcano-sedimentary sequence from the Isle of Mull, North Atlantic Igneous Province. *Lithos*, **482**, 107729, https://doi.org/10.1016/j.lithos.2024.107729

Parfitt, E.A. and Wilson, L. 1999. A Plinian treatment of fallout from Hawaiian lava fountains. *Journal of Volcanology and Geothermal Research*, **88**, 67–75, https://doi.org/10.1016/S0377-0273(98)00103-6

Passey, S.R. and Bell, B.R. 2007. Morphologies and emplacement mechanisms of the lava flows of the Faroe Islands Basalt Group, Faroe Islands, NE Atlantic Ocean. *Bulletin of Volcanology*, **70**, 139–156, https://doi.org/10.1007/s00445-007-0125-6

Patrick, M.R., Houghton, B.F. *et al.* 2020. The cascading origin of the 2018 Kīlauea eruption and implications for future forecasting. *Nature Communications*, **11**, 5646, https://doi.org/10.1038/s41467-020-19190-1

Pedersen, G.B.M., Höskuldsson, A. *et al.* 2017. Lava field evolution and emplacement dynamics of the 2014–2015 basaltic fissure eruption at Holuhraun, Iceland. *Journal of Volcanology and Geothermal Research*, **340**, 155–169, https://doi.org/10.1016/j.jvolgeores.2017.02.027

Peterson, D.W. and Tilling, R.I. 1980. Transition of basaltic lava from pahoehoe to aa, Kilauea Volcano, Hawaii: field observations and key factors. *Journal of Volcanology and Geothermal Research*, **7**, 271–293.

Peterson, D.W., Holcomb, R.T., Tilling, R.I. and Christiansen, R.L. 1994. Development of lava tubes in the light of observations at Mauna Ulu, Kilauea Volcano, Hawaii. *Bulletin of Volcanology*, **56**, 343–360.

Pugsley, J. 2021. *The Stratigraphic Architecture & Evolution of the North-west Mull Lava Field, Isle of Mull, Scotland*. PhD thesis, University of Aberdeen.

Pyle, D.M. 1989. The thickness, volume and grainsize of tephra fall deposits. *Bulletin of Volcanology*, **51**, 1–15.

Quirie, A.K., Schofield, N. *et al.* 2019. The Rattray Volcanics: Mid-Jurassic fissure volcanism in the UK Central North Sea. *Journal of the Geological Society, London*, **176**, 462–481, https://doi.org/10.1144/jgs2018-151

Quirie, A.K., Schofield, N. *et al.* 2020. Palaeogeographical evolution of the Rattray Volcanic Province, Central North Sea. *Journal of the Geological Society, London*, **177**, 718–737, https://doi.org/10.1144/jgs2019-182

Rawlings, D.J., Watkeys, M.K. and Sweeney, R.J. 1999. Peperitic upper margin of an invasive flow, Karoo flood basalt province, northern Lebombo. *South African Journal of Geology*, **102**, 377–383.

Reidel, S.P. 2015. Igneous rock associations 15. The Columbia River basalt group: a flood basalt province in the Pacific Northwest, USA. *Geoscience Canada*, **42**, 151–168, https://doi.org/10.12789/geocanj.2014.41.061

Reidel, S.P and Tolan, T.L. 1992. Eruption and emplacement of flood basalt: an example from the large-volume Teepee Butte Member, Columbia River Basalt Group. *Geological Society of America Bulletin*, **104**, 1650–1671, https://doi.org/10.1130/0016-7606(1992)104<1650:EAEOFB>2.3.CO;2

Reynolds, P., Brown, R.J., Thordarson, T. and Llewellin, E.W. 2015. Rootless cone eruption processes informed by dissected tephra deposits and conduits. *Bulletin of Volcanology*, **77**, 72, https://doi.org/10.1007/s00445-015-0958-3

Reynolds, P., Brown, R.J., Thordarson, T. and Llewellin, E.W. 2016. The architecture and shallow conduits of Laki-type pyroclastic cones: insights into a basaltic fissure eruption. *Bulletin of Volcanology*, **78**, 1–18, https://doi.org/10.1007/s00445-016-1029-0

Richey, J.E. 1961. *British Regional Geology: the Tertiary Volcanic Districts of Scotland*. HMSO.

Ritchie, J.D. and Hitchin, K. 1996. Early Paleogene offshore igneous activity to the northwest of the UK and its relationship to the North Atlantic Igneous Province. *Geological Society, London, Special Publications*, **101**, 63–78.

Rossi, M.J. 1997. Morphology of the 1984 open-channel lava flow at Krafla volcano, northern Iceland. *Geomorphology*, **20**, 95–112.

Sánchez, M.C., Sarrionandia, F., Arostegui, J., Eguiluz, L. and Ibarguchi, J.G. 2012. The transition of spatter to lava-like body in lava fountain deposits: features and examples from the Cabezo Segura volcano (Calatrava, Spain). *Journal of Volcanology and Geothermal Research*, **227**, 1–14.

Schofield, N. and Jolley, D.W. 2013. Development of intra-basaltic lava-field drainage systems within the Faroe–Shetland Basin. *Petroleum Geoscience*, **19**, https://doi.org/10.1144/petgeo2012-061

Self, S., Thordarson, T., Keszthelyi, L., Walker, G.P.L., Hon, K., Murphy, M.T., Long, P. and Finnemore, S. 1996. A new model for the emplacement of

Downloaded from https://www.lyellcollection.org by Guest on Jul 10, 2025

Columbia River basalts as large, inflated pahoehoe lava flow fields. *Geophysical Research Letters*, **23**, 2689–2692.

Self, S., Keszthelyi, L. and Thordarson, T. 1998. The importance of pāhoehoe. *Annual Review of Earth and Planetary Sciences*, **26**, 81–110, https://doi.org/10.1146/annurev.earth.26.1.81

Self, S., Jay, A.E., Widdowson, M. and Keszthelyi, L.P. 2008. Correlation of the Deccan and Rajahmundry Trap lavas: are these the longest and largest lava flows on Earth? *Journal of Volcanology and Geothermal Research*, **172**, 3–19, https://doi.org/10.1016/j.jvolgeores.2006.11.012

Shorttle, O., Maclennan, J. and Lambart, S. 2014. Quantifying lithological variability in the mantle. *Earth and Planetary Science Letters*, **395**, 24–40, https://doi.org/10.1016/j.epsl.2014.03.040

Skogseid, J., Pedersen, T., Eldholm, O. and Larsen, B.T. 1992. Tectonism and magmatism during NE Atlantic continental break-up: the Vøring Margin. *Geological Society, London, Special Publications*, **68**, 305–320.

Stothers, R.B., Wolff, J.A., Self, S. and Rampino, M.R. 1986. Basaltic fissure eruptions, plume heights, and atmospheric aerosols. *Geophysical Research Letters*, **13**, 725–728.

Sumner, J.M., Blake, S., Matela, R.J. and Wolff, J.A. 2005. Spatter. *Journal of Volcanology and Geothermal Research*, **142**, 49–65, https://doi.org/10.1016/j.jvolgeores.2004.10.013

Swanson, D.A., Wright, T.L. and Helz, R.T. 1975. Linear vent systems and estimated rates of magma production and eruption for the Yakima Basalt on the Columbia Plateau. *American Journal of Science*, **275**, 877–905, https://doi.org/10.2475/ajs.275.8.877

Tarquini, S., de'Michieli Vitturi, M., Jensen, E.H., Pedersen, G.B., Barsotti, S., Coppola, D. and Pfeffer, M.A. 2018. Modeling lava flow propagation over a flat landscape by using MrLavaLoba: the case of the 2014–2015 eruption at Holuhraun, Iceland. *Annals of Geophysics*, **61**, 1–18, https://doi.org/10.4401/ag-7812

Thordarson, T. and Self, S. 1993. The Laki (Skaftár fires) and Grímsvötn eruptions in 1783–1785. *Bulletin of Volcanology*, **55**, 233–263.

Thordarson, T. and Self, S. 1998. The Roza Member, Columbia River Basalt Group: a gigantic pahoehoe lava flow field formed by endogenous processes? *Journal of Geophysical Research: Solid Earth*, **103**, 27411–27445.

Tolan, T.L., Martin, B.S., Reidel, S.P., Anderson, J.L., Kindsey, K.A. and Burt, W. 2009. An introduction to the stratigraphy, structural geology, and hydrogeology of the Columbia River Flood Basalt Province: a primer for the GSA Columbia River Basalt Group Field Trips. *In*: O'Connor, J.E., Dorsey, R.J. and Madin, I.P. (eds) *Volcanoes to Vineyards – Geologic Field Trips through the Dynamic Landscape of the Pacific Northwest*. *GSA Field Guide*, **15**, 599–645.

Valentine, G.A. and Gregg, T.K.P. 2008. Continental basaltic volcanoes–processes and problems. *Journal of Volcanology and Geothermal Research*, **177**:857–873 https://doi.org/10.1016/j.jvolgeores.2008.01.050

Valentine, G.A. and Groves, K.R. 1996. Entrainment of country rock during basaltic eruptions of the Lucero volcanic field, New Mexico. *The Journal of Geology*, **104**, 71–90, https://doi.org/10.1086/629802

Vallance, J.W. and Iverson, R.M. 2015. Lahars and their deposits. *In*: Sigurdsson, H. (ed.) *The Encyclopedia of Volcanoes*. Academic Press, 649–664.

Walker, G.P. 1971. Compound and simple lava flows and flood basalts. *Bulletin Volcanologique*, **35**, 579–590, https://doi.org/10.1007/BF02596829

Walker, G.P. 1995. Flood basalts versus central volcanoes and the British Tertiary Volcanic Province. *Geological Society of London, Memoirs*, **16**, 195–202.

Walker, S.N. and Cortés, J.A. 2024. Pāhoehoe lava emplacement in Lon Reudle, Mull. *Scottish Journal of Geology*, **60**, sjg2023-019, https://doi.org/10.1144/sjg2023-019

Wantim, M.N., Suh, C.E., Ernst, G.G.J., Kervyn, M. and Jacobs, P. 2011. Characteristics of the 2000 fissure eruption and lava flow fields at Mount Cameroon volcano, West Africa: a combined field mapping and remote sensing approach. *Geological Journal*, **46**, 344–363, https://doi.org/10.1002/gj.1277

Watson, J. 1977. The Outer Hebrides: a geological perspective. *Proceedings of the Geologists' Association*, **88**, 1–14, https://doi.org/10.1016/S0016-7878(77)80001-1

Wentworth, C.K. 1922. A scale of grade and class terms for clastic sediments. *The Journal of Geology*, **30**, 377–392.

White, R.S. 1993. Melt production rates in mantle plumes. *Philosophical Transactions of the Royal Society of London. Series A: Physical and Engineering Sciences*, **342**, 137–153.

Williamson, I.T. and Bell, B.R. 2012. The Staffa Lava Formation: graben-related volcanism, associated sedimentation and landscape character during the early development of the Palaeogene Mull lava field, NW Scotland. *Scottish Journal of Geology*, **48**, 1–46, https://doi.org/10.1144/0036-9276/01-439

Wilmoth, R.A. and Walker, G.P. 1993. P-type and S-type pahoehoe: a study of vesicle distribution patterns in Hawaiian lava flows. *Journal of Volcanology and Geothermal Research*, **55**, 129–142, https://doi.org/10.1016/0377-0273(93)90094-8

Wilson, L. and Walker, G.P.L. 1987. Explosive volcanic eruptions – VI. Ejecta dispersal in plinian eruptions: the control of eruption conditions and atmospheric properties. *Geophysical Journal International*, **89**, 657–679.

Wolfe, W.E., Neal, A.C., Banks, G.N. and Toni, D.J. 1988. *The Puu Oo eruption of Kilauea volcano, Hawaii: episodes 1 through 20, January 3, 1983, through June 8, 1984*. US Geological Survey, Professional Papers, **1463**.